A Synthetic Coiled-Coil Interactome Provides Heterospecific Modules for Molecular Engineering

A synthetic coiled-coil interactome provides heterospecific modules for molecular engineering

Aaron W. Reinke, Robert A. Grant and Amy E. Keating
MIT Department of Biology
77 Massachusetts Avenue
Cambridge, MA 02139
keating@mit.edu

Abstract

The versatile coiled-coil protein motif is widely used to induce and control macromolecular interactions in biology and materials science. Yet the types of interaction patterns that can be constructed using known coiled coils are limited. Here we greatly expand the coiled-coil toolkit by measuring the complete pair-wise interactions of 48 synthetic coiled coils and 7 human bZIP coiled coils using peptide microarrays. The resulting 55-member protein 'interactome' includes 27 pairs of interacting peptides that preferentially hetero-associate. The 27 pairs can be used in combinations to assemble sets of 3 to 6 proteins that compose networks of varying topologies. Of special interest are heterospecific peptide pairs that participate in mutually orthogonal interactions. Such pairs provide the opportunity to dimerize two separate molecular systems without undesired crosstalk. Solution and structural characterization of two such sets of orthogonal heterodimers provide details of their interaction geometries. The orthogonal pair, along with the many other network motifs discovered in our screen, provide new capabilities for synthetic biology and other applications.

The coiled coil is a fundamental building block for molecular engineering. Its simple structure, which consists of two or more alpha helices twisted into a supercoiled rod-like bundle, is encoded in a seven amino-acid repeat designated [**abcdefg**]$_n$. Coiled coils have been used to induce and stabilize protein oligomers, to promote protein-protein interactions, to rewire cellular networks, to assemble functional scaffolds, to construct hydrogel materials, and to self-assemble nano-scale fibers and/or recruit ligands to nanopartices[1-9]. Important early advances in coiled-coil engineering included demonstrating that leucine-zipper peptides, which are short coiled coils of ~40 amino acids, can fold to give stable structures composed of two to four helices, and that coiled coils can be modified using charge patterning to encode heterospecificity and helix orientation[10]. In particular, peptide "Velcro" is a designed heterospecific coiled-coil dimer with glutamates at all interfacial **e** and **g** positions on one helix and lysines at all **e** and **g** positions on the other; this heterodimer and variants of it have been widely employed in bio-molecular engineering. Further experiments have illustrated how residues at the hydrophobic interface, particularly those in **a** positions, can be mutated to modulate interaction affinity and introduce additional specificity[11]. Prior studies not only generated reagents that have found many uses, but also elucidated structural principles that control interaction selectivity[12-14].

Heterodimeric coiled-coil pairs have proven particularly useful for molecular engineering[12-18]. Exciting recent applications have included using coiled-coil heterodimers to modulate MAP kinase signaling in yeast and inducing ordered structure via coiled coils in nano-scale fibers. Notably, while coiled-coil reagents for inducing homo-oligomerization or hetero-oligomerization of single complexes are widely used, the modern coiled-coil toolkit does not provide access to more complex interaction patterns. Lacking is a large set of coiled coils that participate in specific and defined interactions with one another. Such reagents could be used to construct interaction networks containing multiple associations in a logical manner. For example, when engineering cellular circuits it might be desirable to implement multiple parallel pathways, each using coiled coils to direct assembly of signaling complexes without crosstalk. Likewise, to engineer artificial transcription factors, heterodimers with specified cross-interactions could provide access to combinatorial control of binding to different DNA sites. For

complex applications such as these, greater versatility is required than is currently provided by characterized coiled-coil peptides.

Results and Discussion

We recently reported the computational design of synthetic peptides that interact with the coiled-coil regions of human bZIP transcription factors. These designed peptides are 35-54 residues in length and share an amino-acid composition characteristic of bZIP leucine zippers (Figure S1, Table S1). Homodimerization of the designed peptides was disfavored by a variety of strategies, and experiments confirmed that most designs do not form strong self-associations[19]. Speculating that this set of heterospecific reagents might harbor interesting and useful interactions patterns, we systematically measured all pair-wise interactions involving 48 designed peptides and 7 additional coiled coils from human bZIPs that do not strongly self-associate.

To identify new heterospecific coiled-coil interactions in a high-throughput manner, we used a protein microarray assay. A complete 55 x 55 interaction matrix was generated by spotting small amounts of each peptide onto aldehyde-derivatized slides (Figure S2, Table S2). Each of the 55 proteins in turn was labeled with Cy3 dye and used in solution to probe subarrays printed on the slides. This assay is highly reproducible and shows good reciprocity with respect to which protein is immobilized (Figures S2 and S3). The relative ordering of fluorescence intensities on the arrays has also been shown to agree qualitatively with solution stability measurements[19,20].

To discover new pairs of hetero-associating coiled coils, the interaction matrix was examined for peptides that: (1) did not show evidence of homo-association and (2) made strong, reciprocal interactions with a partner. Interacting and non-interacting pairs were chosen conservatively based on comparisons of prior array data with solution data. A total of 27 heterospecific pairs involving 23 synthetic peptides (named SYNZIPs 1-23) and 3 human bZIPs were selected for further analysis (Figure 1).

Coiled coils can vary in their oligomerization state, helix orientation and axial helix alignment[21]. For the heterospecific pairs uncovered in this assay to be maximally useful, knowledge of their interaction geometry is important. The synthetic coil-coiled peptides were designed to interact with individual human bZIPs as parallel dimers, and we hypothesize that most of the design-design and design-human complexes detected on the arrays also form parallel dimers. Several lines of evidence support this. First is the special role of paired **a**-position asparagines in leucine zippers. Interaction of an

asparagine residue with another asparagine on an opposing helix is common in coiled-coil dimers and is much more favorable than an interaction with a hydrophobic residue (which we term an "Asn mismatch," unless the Asn occurs very close to the end of the coiled coil)[10, 11]. Paired asparagines at **a** favor parallel dimer formation and are strongly conserved in the parallel, dimeric leucine-zipper transcription factors[10, 13, 22]. Almost all (23 out of 26) peptides analyzed here contain at least one Asn residue at a coiled-coil **a** position, and of the 27 heterospecific pairs considered, 24 can be aligned such that two **a**-position Asn residues are paired. All heterospecific pairs can be aligned as parallel dimers without any Asn mismatches[11]. In addition to the role of Asn residues, half of the 26 peptides also include a charged residue in one or two non-terminal **a** positions. Lysine in **a** positions has been reported to favor dimer formation over higher order oligomerization, presumably because **a** positions in dimers are less buried[10, 23]; this likely applies for other charged side chains as well, as is supported by the lower frequencies of Lys, Arg and Glu residues in **a** positions of parallel trimers compared to parallel dimers (K. Gutwin and A. Keating, unpublished data). Additional indirect criteria support parallel dimer formation. For example, when considered as parallel dimers, all pairs can be aligned such that net **g-e'** electrostatic interactions are not unfavorable and destabilizing[10, 14]. Finally, none of the heterospecific interactions encode a motif that has been reported to favor trimer formation[24].

Given 27 heterospecific pairs among 26 peptides that likely form parallel coiled-coil dimers, we analyzed these to identify higher-order patterns of interaction and non-interaction. Each of the 26 peptides participates in 1-7 interactions, suggesting that subnetworks involving more than 2 peptides could be common in our data (Figure 1). We searched exhaustively for all subnetworks containing 3-6 proteins and found examples of the 10 topologies shown in Figure 2A (Table S3)[25]. In that figure, an edge indicates a high-confidence observation of an interaction on the array and the absence of an edge indicates that an interaction was not observed. Most networks are based on motifs we describe as "pair", "line", or "hub" structures. Many networks are composed of smaller networks, such as the 4 node "orthogonal pair" (2 pairs with no cross-interactions), "orthogonal triplet" (3 pairs with no cross-interactions) or the 5 node "pair + line" (similarly with no cross interactions). Interestingly, protein nodes in the networks are sparsely connected. It may be that features engineered to diminish self-association also reduce interaction promiscuity more broadly.

Because of its immediate utility, e.g. for direct extension of existing applications, we chose the orthogonal-pair motif for further characterization[1, 2, 6]. Three coiled-coil pairs were selected that participate in two sets of orthogonal interactions. All three pairs were evaluated in solution using circular dichroism (Figure 2B and C, Figure S4). The six individual peptides gave only weak helical signal in isolation. But mixing each peptide with its appropriate partner gave a spectrum characteristic of a coiled coil, confirming heterospecific interaction. The orthogonal sets that can be constructed from these three pairs each consist of four peptides that participate in two interactions ('on' states) and eight non-interactions ('off' states). We measured the thermal stabilities of the ten possible interactions for each set (Figure 2D and E, Figure S5). The 'on' states had melting temperatures between 32 and 47 °C, at 8 μM total peptide concentration. For [SYNZIP6:SYNZIP5, SYNZIP1:SYNZIP2] the difference between the weakest 'on' state and the strongest 'off' state was ~8 °C. For [SYNZIP4:SYNZIP3, SYNZIP1:SYNZIP2] the difference was ~18 °C. (See Figure S6 for characterization of an additional orthogonal set.) Previously published orthogonal coiled-coil pairs are either much less stable than this, have the property that at least one 'off' interactions is more stable than one 'on' interaction, or incorporate non-natural amino acids[15-17, 26].

To confirm the interaction geometry of complexes composing the orthogonal pairs, we solved the structures of SYNZIP6:SYNZIP5 and SYNZIP1:SYNZIP2 to 2.5 and 1.8 Å, respectively (Figure S7, Table S4). Both complexes are parallel heterodimers, as anticipated (Figure 3A and B). We were unable to obtain crystals of SYNZIP4:SYNZIP3. While it is likely that this pair forms a parallel dimer (it includes **a**-position Asn and Lys residues and highly charged **e**- and **g**-position residues), SYNZIP3 is shorter than SYNZIP4, and the precise axial alignment of its two helices is uncertain. Either of two Asn residues in SYNZIP4 could be paired with the single **a**-position Asn in SYNZIP3, while maintaining a similar extent of coiled-coil dimer. To experimentally determine the alignment, two truncated versions of SYNZIP4 were generated. Each was mixed with SYNZIP3, and the thermal stabilities of the resulting complexes were measured by CD. The N-terminal SYNZIP4 truncation had very similar stability to the full-length peptide, while the C-terminal truncation was markedly destabilized (Figure 3C). Thus, the two most N-terminal heptads of SYNZIP4 are dispensable for the interaction. Based on these experiments, helical wheel diagrams were generated for the three heterospecific pairs (Figure 3 D-F).

These experiments suggested that portions of each complex were dispensable for the formation of orthogonal pairs. To demonstrate that shorter experimentally determined interaction regions interact specifically, truncated versions of SYNZIPs 1-6 (shown in Figure 3 D-F) were cloned with an N-terminal cysteine. Each protein was labeled with biotin. SYNZIPs 1 and 2 were also labeled with Alexa Fluor 546, and SYNZIPs 3, 4, 5, and 6 were labeled with Alexa Fluor 488. For each orthogonal set, each biotinylated protein was pre-mixed with the three other fluorescent proteins and then incubated with NeutrAvidin coated beads. These pull-down experiments showed that each biotinylated protein interacted specifically with its cognate partner (Figure 4A and B). Thus, the shorter peptides are sufficient to form specific interactions in four-component mixtures.

The crystal structures of SYNZIP6:SYNZIP5 (PDB ID 3HE4) and SYNZIP1:SYNZIP2 (PDB ID 3HE5) reveal interactions involving polar and charged residues that likely play a role in encoding specificity. Both structures include paired asparagines at **a-a'** positions that adopt conformations seen frequently in other parallel coiled-coil dimers. Neither structure contains any asparagine mismatches at non-terminal heptad positions, although both have mismatches at the extreme N-terminal heptad. At that position, asparagine is paired with valine but remains largely solvent exposed due to its location at the end of the helix. In the SYNZIP6:SYNZIP5 complex, in both the fourth and fifth heptads, Lys at **a** across from Ile interacts with an aspartate at the proceeding **g'** position (Figure 3G). In the SYNZIP1:SYNZIP2 complex, the fourth heptad contains a complex polar network involving a partly buried water molecule. The water is coordinated by SYNZIP1 residues Asn 24 at **a** and Lys 27 at **d**, as well as by SYNZIP2 residue Glu 24 at **a'**. In the 3 copies of the heterodimer in the asymmetric unit, Lys 23 at **g** on SYNZIP1, as well as Gln 25 at **b'** and Glu 28 at **e'** on SYNZIP2, are involved to varying degrees in this extended network (Figure 3H). These interactions suggest that charged residues in coiled-coil core positions can contribute specificity in parallel dimers, although such residues may be accommodated in ways that are difficult to anticipate, as illustrated here by incorporation of a water molecule.

It is interesting to speculate about how specificity in the orthogonal sets is determined. The simple ACID-BASE charge repulsion strategy used in peptide "Velcro" is not sufficient to encode complex interaction patterns in coiled coils only ~40 amino acids long. How are so many different 'off' states disfavored? Using a simple model, 5 of the 14 'off' pairs among the two orthogonal pair sets have net repulsive electrostatic

interactions at **g-e'** positions, when considered as parallel dimers. Unavoidable Asn mismatches appear in an additional 2 pairs. In the remainder, charged residues at **a** and **d** positions appear important, with **a**-position Lys and Glu residues disfavoring homodimerization, and repulsive charges at **g-a'** and **d-e'** pairs disfavoring both homo- and heterodimers[11]. All of these interactions are implicated as useful and important negative design features. In terms of improving specificity, if this is required, we stress that the undesired complexes that form are weak and are not necessarily parallel dimers.

The orthogonal pairs introduced here dramatically increase the number of small, heterospecific protein-protein interaction partners that can be used as modular components for molecular engineering[27]. The peptides can be over-expressed in *Escherichia coli*, contain aromatic amino acids for quantification using spectrometry and lack cysteines. While most of these peptides do partner with human bZIPs, they are likely to be effective for applications in yeast or bacteria, where human orthologs are absent, as well as *in vitro* and for materials applications. These reagents, or molecular parts, are also likely to be useful when paired with other types of synthetic or native interaction domains such as zinc fingers[28]. It is reasonable to consider using them to design novel transcription factors that do not cross-interact, or to elaborate molecular scaffolds[1, 6]. Finally, the large number of interactions measured in the course of characterizing these peptides will be useful for testing computational models and further understanding the interaction specificity of "simple" coiled coils.

Methods and Materials

Plasmid construction, protein expression and purification

Proteins used in the array experiments were cloned, expressed and purified as published previously[19]. For solution studies and crystallography, genes were cloned into pSV282 (Vanderbilt University Medical Center, Center for Structural Biology) using BamHI and XhoI restriction enzymes (NEB). For the pull-down assays, synthetic genes for truncated peptides including an N-terminal cysteine and a short linker (GSCGS) were cloned based on experimentally determined alignments. SYNZIP6 was mutated at a **c**-position lysine to include a tyrosine for concentration determination. Each plasmid was transformed into RP3098 cells and 1 L cultures in LB were grown to 0.4-0.6 OD and induced at 37 °C for 3-4 hours with the addition of 1mM IPTG. MBP fusion proteins with a His_6 tag were purified under native conditions by binding to Ni-NTA resin (Qiagen) and eluting with 8

ml elution buffer (300 mM imidazole, 20 mM Tris, 500 mM NaCl, 1mM DTT, pH 7.9). Fusion proteins were then dialyzed overnight at 4 °C in TEV cleavage buffer (50 mM Tris, 50 mM NaCl, 1 mM DTT, 0.5 mM EDTA, pH 7.5). Peptides were cleaved from MBP by incubating with 100 µl TEV protease (1mg/ml) for 3 hours at room temp. After cleavage, the mixture was added to Ni-NTA resin and the flow through was collected. In the case of SYNZIP2, the peptide bound the Ni-NTA resin after cleavage. SYNZIP2 was eluted from the resin with 6 M guanidine-HCl and the elute was then dialyzed into water. Peptides were additionally purified using reverse-phase HPLC and lyophilized. The molecular weights of the peptides were confirmed by mass spectrometry. Protein concentrations were determined using the Edelhoch method[29] of UV absorbance at 280 in 6 M guanidine-HCl/100 mM sodium phosphate pH 7.4. Protein and DNA sequences are listed in Table S1.

Coiled-coil array assay

All array experiments were carried out as previously published[19], with the exception that only two spots for each protein were printed per subarray, for a total of 8 measurements of each heteromeric interaction. Briefly, lyophilized proteins were resuspended to a concentration of 40 µM in 6 M guanidine-HCl/100 mM sodium phosphate pH 7.5/0.04% Triton X-100/10 µM Alexa Fluor 633 hydrazide. Proteins were printed on aldehyde-derivatized glass slides and 12 identical subarrays per slide were physically divided by drawing a hydrophobic boundary. Slides were blocked, and then each subarray was probed with Cy3-labeled proteins diluted six-fold from 6 M guanidine-HCl/100 mM sodium phosphate pH 7.5/6 mM TCEP to a concentration of ~160 nM in 1.2X buffer (1.2% BSA, 1.2X PBS, 0.12% Tween-20). Slides were then washed, dried, and scanned to obtain fluorescence values for each spot. Average background-corrected fluorescence values are listed in Table S2**.**

Data analysis

For each peptide pair, fluorescence intensities for the 4 replicate spots corresponding to the same surface/solution arrangement were corrected for background and then averaged. Averages were corrected further by subtracting the median signal for all proteins on the surface interacting with the same solution probe; this gave a value F. The quantity *arrayscore* was calculated by taking $-\log(F/F_{max})$ where F_{max} was the maximum F value

for a given solution probe. To identify heterospecific pairs, a strict criterion was employed by comparing *arrayscore* values to T_m measurements of previously published data[19]. Non-interactions were required to have *arrayscore* > 1, which corresponds to an average T_m of 14 °C (based on 13 comparisons). Interactions were required to have *arrayscore* < 0.2, which corresponds to an average T_m of 43 °C (based on 7 comparisons). These same criteria for interactions and non-interactions were employed to identify subnetworks when using Fanmod [25] to search for all possible 3-6 node networks. Motifs are listed in Table S3**.**

Circular dichroism

Circular dichroism spectra were measured on an AVIV 400 spectrometer in 12.5 mM potassium phosphate (pH 7.4)/150 mM KCl. Individual measurements were made at 4 μM peptide or 4 μM of each peptide (8 μM total peptide) for mixtures. All measurements were made in a 1 cm cuvette. Mixtures of peptides were incubated for several hours at room temperature before measurement. Spectra were measured at 25 °C. Wavelength scans were monitored from 280 nm to 195 nm in 1 nm steps, averaging for 5 seconds at each wavelength. Three scans for each sample were averaged. Thermal unfolding curves were performed at 4 μM peptide for individual measurements or 4 μM of each peptide (8 μM total peptide) for mixtures and measured in a 1 cm cuvette with stirring. Melting curves were determined by monitoring ellipticity at 222 nm with an averaging time of 30 seconds, an equilibration time of 1.5 minutes, and a scan rate of 2 °C/min. All samples were measured from 0 to 85 °C. T_m values were estimated as reported previously[19]. All thermal denaturations were reversible, with differences in T_m values upon folding vs. unfolding of < 2°C for all but 2 weak complexes, and < 5 °C in all cases.

For a third orthogonal set of coiled-coil heterodimers, a slightly modified CD protocol was employed. The CD spectra in Figure S6 were measured on an Aviv Model 202 spectrometer in 12.5 mM potassium phosphate (pH 7.4)/150 mM KCl. Individual measurements were made at 40 μM peptide and mixtures at 20 μM of each peptide, 40 μM total peptide. Mixtures of peptides were incubated for several hours at room temperature before measurement. Spectra were measured at 25 °C. Wavelength scans were performed in a 0.1 cm cuvette and were monitored from 260 nm to 195 nm in 1 nm steps averaging for 5 seconds at each wavelength.

Crystallography

Purified lyophilized protein was re-suspended in water to a concentration of 20 mg/ml and mixed to give 20 mg/ml of each complex. Crystals were grown by the hanging drop method at room temperature by mixing 1 µl protein solution with 1 µl of reservoir solution. SYNZIP1:SYNZIP2 was grown in 45% MPD, 100 mM Tris pH 8.0, and 160 mM ammonium acetate. SYNZIP6:SYNZIP5 was grown in 100 mM Tris pH 8.2 and 20% MPD. Crystals were frozen in LN2 without addition of any cryoprotectant. Diffraction data were collected at 100K on a Rigaku MicroMax007-HF with VariMax-HR optics and a RAXIS-IV detector (SYNZIP1: SYNZIP2) or at the NE-CAT 24ID-E beam line of the Advanced Photon Source (SYNZIP6:SYNZIP5) and processed using HKL2000[30]. Both structures were solved by molecular replacement using PHASER[4]. In each case the search model was derived from a single energy-minimized theoretical model selected from an ensemble of models spanning the space of parameters of native parallel dimeric coiled-coil structures. The ensemble was generated as previously described[5]. The search models had no overhangs and the side chains at all non-interfacial positions (**b**, **c**, and **f**) were truncated to alanine. Model building was done using COOT[31, 32] using twin law corrections for both structures (Table S4). Non-crystallographic symmetry (NCS) restraints between the four copies of the heterodimer in the asymmetric unit (ASU) of the SYNZIP6:SYNZIP5 crystals were used to aid in the refinement of that structure. Geometry was checked using MOLPROBITY[33] and no outliers were identified (Table S4). Figures of structures were generated using PyMol (DeLano Scientific, Palo Alto, CA).

Pull down assay

Proteins containing a unique N-terminal cysteine were labeled by mixing 100 µM protein with 0.5 mM Alexa Fluor 488 or 546 maleimide (Invitrogen) or 2 mM maleimide-PEG11-biotin (Thermo Scientific) in 100 mM potassium phosphate pH 7.0/150 mM KCl/1 mM TCEP. Solutions were incubated for three hours at 18-22 °C. Free dye or biotin was removed using desalting spin columns (Thermo Scientific). Biotinylated proteins were concentrated using centrifugal filter units (Millipore). The concentration of unlabeled and biotinylated proteins was determined using the Edelhoch method. The concentration of dye labeled proteins was estimated by assuming a 50% recovery after desalting. Each dye labeled protein was mixed with the unlabeled version (at known

concentration) in a 1:10 ratio. 400 pmoles of each protein indicated in Figure 4 were mixed in 75 µl binding buffer (12.5 mM potassium phosphate pH 7.4, 150 mM KCl, 1 mM DTT, 1% BSA, 0.1% Tween-20). Protein mixtures were incubated for 1 hour at 18-22 °C and then 50 µl of a 50% slurry of NeutrAvidin beads (Thermo Scientific) in binding buffer was added. Mixtures were incubated for 2 hours at 18-22 °C with rotation. Beads were then washed 3 times with 1 ml binding buffer at 4 °C and mixed with 100 µl of loading buffer (10 % glycerol, 2% SDS, 100 mM DTT, 0.01% bromophenol blue, 100 mM Tris pH 6.8). Following heating at 65 °C for 15 minutes, 10 µl of each sample was loaded onto an 18% Tris-glycine gel (Invitrogen). Gels were imaged on a Typhoon 9400 imager. Fluorsep software (Amersham Biosciences) was used to remove background fluorescent overlap.

Sequence analysis

Positions **a**-**g** in the coiled-coil heptad repeat were assigned manually, as designed previously[19], based on conserved Leu residues and overall hydrophobic/polar patterning. Each peptide contains 5-7 full heptads. The following criteria were applied for sequence analysis. To predict the most probable alignments of coiled-coil dimers, all possible helix alignments that overlapped by at least 5 full heptads and did not contain an asparagine mismatch were considered. Asparagine mismatches were defined as an Asn residue at a non-terminal **a** position across from isoleucine, valine or leucine at a non-terminal **a** position. A terminal **a** position was defined as an **a** position ≤ 3 residues from the end of the coiled coil. For assessing **g-e'** electrostatics, the least repulsive alignment of ≥ 5 heptads that did not contain an asparagine mismatch was used. For this purpose, each attractive **g-e'** interaction was scored as + 0.5 and each repulsive **g-e'** interaction was scored as -0.5. Negatively charged glutamate and aspartate, and positively charged lysine and arginine were considered during scoring. Note that Glu, Lys, Arg and – to a lesser extent – Asp overwhelmingly predominate at **g** and **e** positions of the 26 peptides considered (Figure S1).

Acknowledgements:

This work was supported by NIH award GM067681. This work is based upon research conducted at the Northeastern Collaborative Access Team beamlines of the Advanced

Photon Source, supported by award RR-15301 from the National Center for Research Resources at the National Institute of Health. Use of the Advanced Photon Source is supported by the U.S. Department of Energy, Office of Basic Energy Sciences, under Contract No. DE-AC02- We thank the MIT BioMicro center for arraying instrumentation, J.R. Apgar for generating models used for structure determination and G. Grigoryan for computational design of synthetic peptides not described elsewhere. We thank members of the Keating laboratory for comments on the manuscript.

Supporting Information Available: Sequences and data for all 55 peptides measured on the protein arrays, additional CD data, crystallographic data and refinement statistics and electron density maps of crystal structures. This information is available free of charge via the Internet at http://pubs.acs.org/.

References

1. Bashor, C. J.; Helman, N. C.; Yan, S.; Lim, W. A. *Science* **2008,** *319*, 1539-1543.
2. Diehl, M. R.; Zhang, K.; Lee, H. J.; Tirrell, D. A. *Science* **2006,** *311*, 1468-1471.
3. Eckert, D. M.; Malashkevich, V. N.; Hong, L. H.; Carr, P. A.; Kim, P. S. *Cell* **1999,** *99*, 103-115.
4. Papapostolou, D.; Smith, A. M.; Atkins, E. D. T.; Oliver, S. J.; Ryadnov, M. G.; Serpell, L. C.; Woolfson, D. N. *Proceedings of the National Academy of Sciences* **2007,** *104*, 10853-10858.
5. Takagi, J.; Erickson, H. P.; Springer, T. A. *Nat Struct Mol Biol* **2001,** *8*, 412-416.
6. Wolfe, S. A.; Grant, R. A.; Pabo, C. O. *Biochemistry* **2003,** *42*, 13401-13409.
7. Petka, W. A.; Harden, J. L.; McGrath, K. P.; Wirtz, D.; Tirrell, D. A. *Science* **1998,** *281*, 389-392.
8. McAllister, K. A.; Zou, H.; Cochran, F. V.; Bender, G. M.; Senes, A.; Fry, H. C.; Nanda, V.; Keenan, P. A.; Lear, J. D.; Saven, J. G.; Therien, M. J.; Blasie, J. K.; DeGrado, W. F. *Journal of the American Chemical Society* **2008,** *130*, 11921.
9. Mapp, A. K.; Ansari, A. Z.; Ptashne, M.; Dervan, P. B. *Proceedings of the National Academy of Sciences of the United States of America* **2000,** *97*, 3930-3935.
10. Mason, J. M.; Muller, K. M.; Arndt, K. M. *Methods Mol Biol* **2007,** *352*, 35-70.
11. Acharya, A.; Rishi, V.; Vinson, C. *Biochemistry* **2006,** *45*, 11324-11332.
12. Arndt, K. M.; Pelletier, J. N.; Müller, K. M.; Plückthun, A.; Alber, T. *Structure* **2002,** *10*, 1235-1248.
13. Moll, J. R.; Ruvinov, S. B.; Pastan, I.; Vinson, C. *Protein Sci* **2001,** *10*, 649-655.
14. O'Shea, E. K.; Lumb, K. J.; Kim, P. S. *Current Biology* **1993,** *3*, 658-667.
15. Lai, J. R.; Fisk, J. D.; Weisblum, B.; Gellman, S. H. *Journal of the American Chemical Society* **2004,** *126*, 10514-10515.
16. Diss, M. L.; Kennan, A. J. *Journal of the American Chemical Society* **2008,** *130*, 1321-1327.
17. Bromley, E. H. C.; Sessions, R. B.; Thomson, A. R.; Woolfson, D. N. *Journal of the American Chemical Society* **2009,** *131*, 928-930.
18. Mason, J. M.; Schmitz, M. A.; Müller, K. M.; Arndt, K. M. *Proceedings of the National Academy of Sciences* **2006,** *103*, 8989-8994.
19. Grigoryan, G.; Reinke, A. W.; Keating, A. E. *Nature* **2009,** *458*, 859-864.
20. Newman, J. R. S.; Keating, A. E. *Science* **2003,** *300*, 2097-2101.
21. Grigoryan, G.; Keating, A. E. *Current Opinion in Structural Biology* **2008,** *18*, 477-483.
22. Harbury, P. B.; Zhang, T.; Kim, P. S.; Alber, T. *Science* **1993,** *262*, 1401-1407.
23. Campbell, K. M.; Sholders, A. J.; Lumb, K. J. *Biochemistry* **2002,** *41*, 4866-4871.
24. Kammerer, R. A.; Kostrewa, D.; Progias, P.; Honnappa, S.; Avila, D.; Lustig, A.; Winkler, F. K.; Pieters, J.; Steinmetz, M. O. *Proceedings of the National Academy of Sciences of the United States of America* **2005,** *102*, 13891-13896.
25. Wernicke, S.; Rasche, F. *Bioinformatics* **2006,** *22*, 1152-1153.
26. Diss, M. L.; Kennan, A. J. *Org Lett* **2008,** *10*, 3797-800.
27. Bromley, E. H. C.; Channon, K.; Moutevelis, E.; Woolfson, D. N. *ACS Chemical Biology* **2008,** *3*, 38-50.
28. Giesecke, A. V.; Fang, R.; Joung, J. K. *Mol Syst Biol* **2006,** *2*, 2006.0011.
29. Edelhoch, H. *Biochemistry* **1967,** *6*, 1948-54.

30. Otwinowski, Z.; Minor, W.; Charles W. Carter, Jr., [20] Processing of X-ray diffraction data collected in oscillation mode. In *Methods in Enzymology*, Academic Press: 1997; Vol. Volume 276, pp 307-326.
31. Emsley, P.; Cowtan, K. *Acta Crystallographica Section D* **2004,** *60*, 2126-2132.
32. Adams, P. D.; Grosse-Kunstleve, R. W.; Hung, L.-W.; Ioerger, T. R.; McCoy, A. J.; Moriarty, N. W.; Read, R. J.; Sacchettini, J. C.; Sauter, N. K.; Terwilliger, T. C. *Acta Crystallographica Section D* **2002,** *58*, 1948-1954.
33. Davis, I. W.; Leaver-Fay, A.; Chen, V. B.; Block, J. N.; Kapral, G. J.; Wang, X.; Murray, L. W.; Arendall, W. B., III; Snoeyink, J.; Richardson, J. S.; Richardson, D. C. *Nucl. Acids Res.* **2007,** *35*, W375-383.

Figures

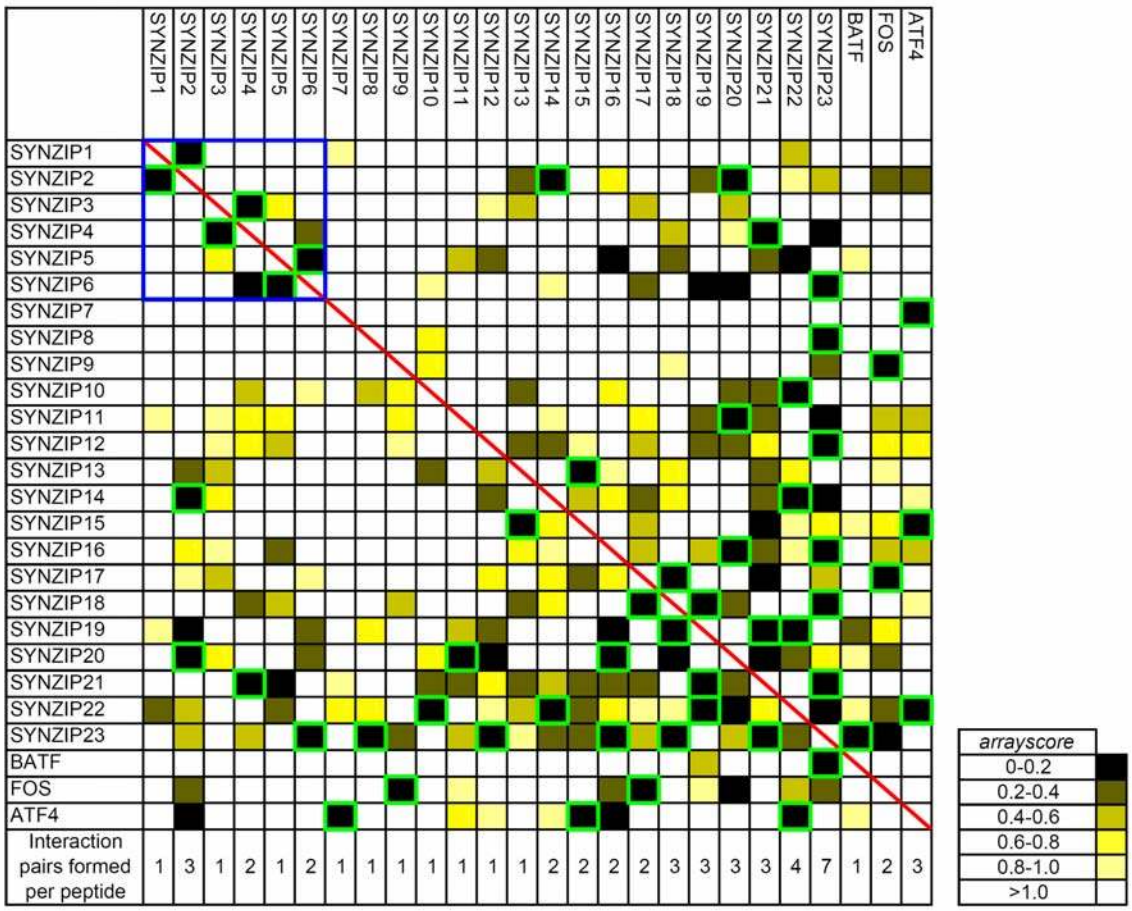

Figure 1. Array data describing the interactions of 26 peptides that form specific interaction pairs. Peptides printed on the surface are listed in rows, and fluorescently labeled peptides in solution are listed in columns. Color indicates the strength of the array fluorescence signal, given as *arrayscore* values (see Methods) according to the color bar at right with 0 (black) indicating the strongest signal and >1 (white) indicating the weakest. SYNZIP peptides 1-6, which are further described in Figures 2-4, are in the top left corner, boxed in blue. The red diagonal highlights the absence of homoassociation of peptides on the arrays. Interactions that showed arrayscore ≤ 0.2 in both measurement directions are boxed in green. The number of strong, reciprocal interactions formed by each peptide is listed at bottom of each column.

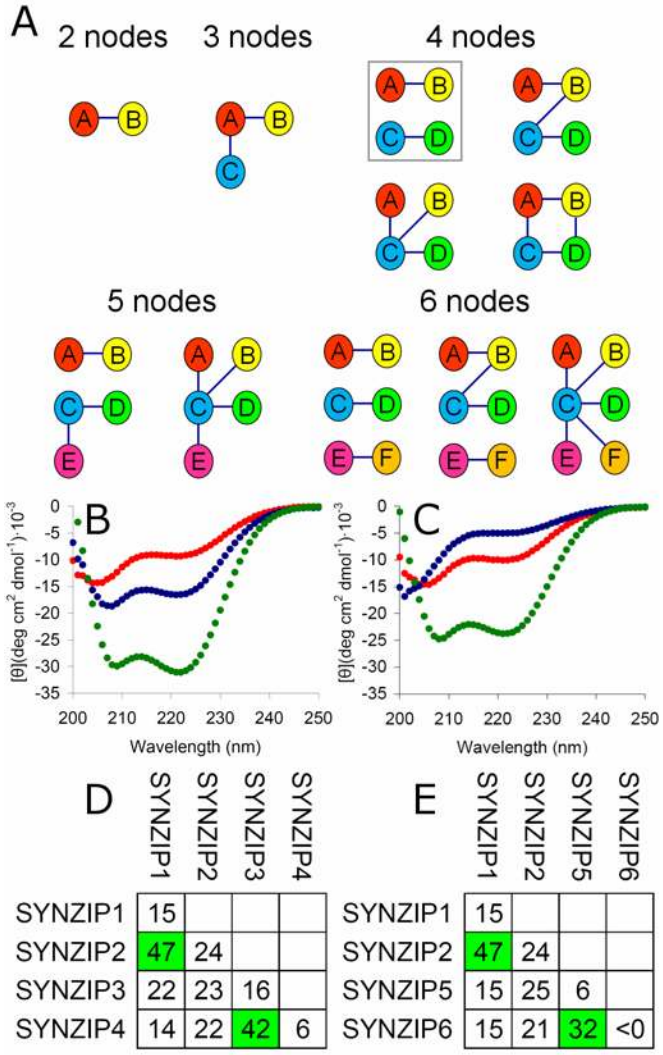

Figure 2. SYNZIP coiled coils form specific interaction subnetworks. (A) Graphical representation of subnetworks detected in the coiled-coil array data. Edges indicate an interaction and the absence of an edge between nodes indicates no interaction in the microarray screen. The orthogonal pair motif is boxed in grey. (B, C) CD spectra for two pairs of heterospecific coiled coils (4 μM of each protein and 8 μM total for mixtures, 25 °C). (B) SYNZIP2 (blue), SYNZIP1 (red), and SYNZIP2 + SYNZIP1 (green). (C) SYNZIP4 (blue), SYNZIP3 (red), and SYNZIP4 + SYNZIP3 (green). (D, E) Melting temperatures (T_ms) derived from fits to thermal melts of peptide mixtures. T_m values for the interacting pair mixtures are highlighted in green.

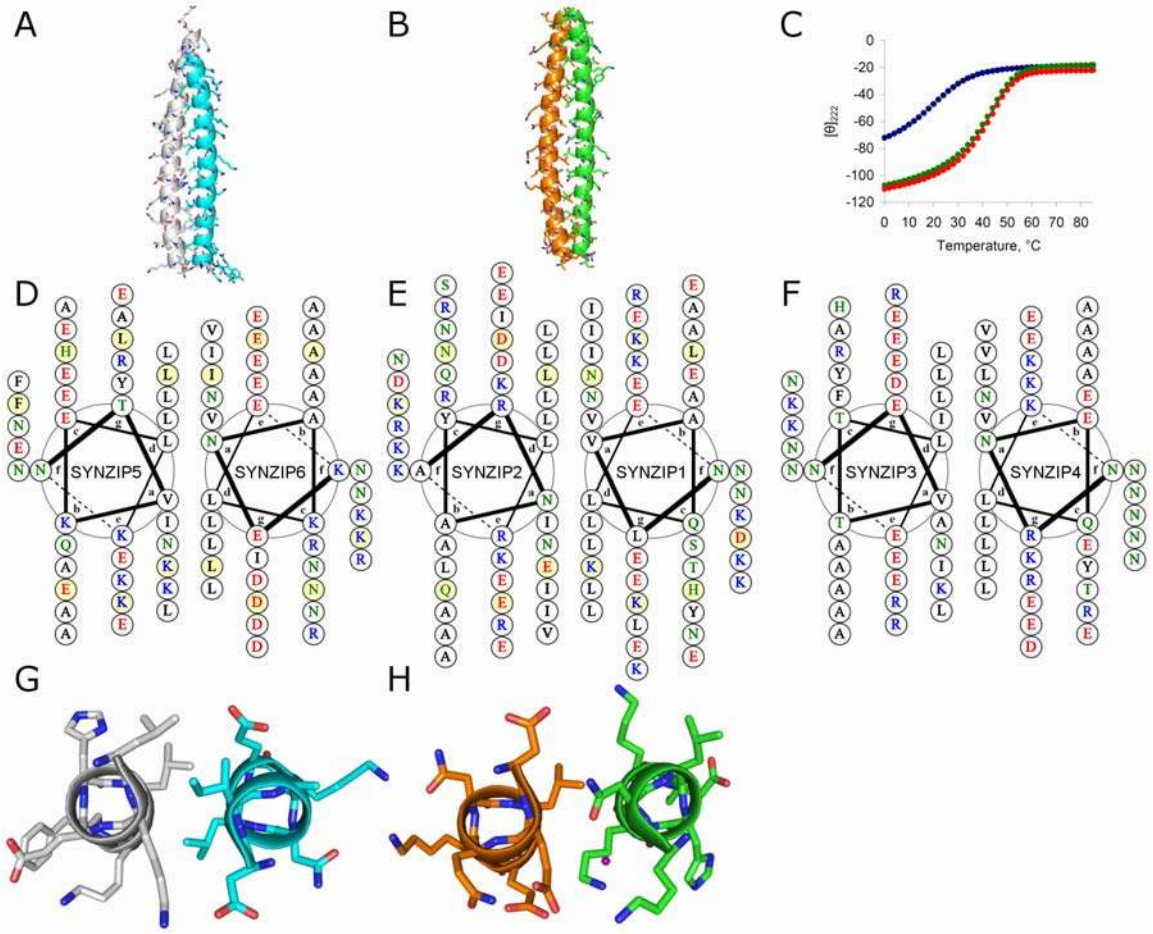

Figure 3. Interaction geometries for three heterospecific SYNZIP pairs. (A, B) Crystal structures of SYNZIP5:SYNZIP6 (A) (grey:teal) and SYNZIP2:SYNZIP1 (B) (orange:green) show that both complexes are parallel coiled-coil heterodimers. (C) Determination of the axial alignment of SYNZIP4:SYNZIP3 using CD thermal melts. $SYNZIP4_{1\text{-}54}$: SYNZIP3 (red), $SYNZIP4_{1\text{-}42}$: SYNZIP3, (blue), and $SYNZIP4_{15\text{-}54}$: SYNZIP3 (green). Each mixture was measured at 8 μM total peptide concentration, 4 μM of each peptide. (D-F) Helical wheel diagrams for SYNZIP5:SYNZIP6 (D), SYNZIP2:SYNZIP1 (E), and SYNZIP3:SYNZIP4 (F). Charged residues are colored red/blue, polar residues are in green, and hydrophobic residues are in black. Residues shaded yellow in (D) and (E) correspond to those shown in panels (G) and (H)**,** respectively. (G) The fourth heptad of SYNZIP5 (residues 23-29):SYNZIP6 (residues 37-

43), and (H) the fourth heptad of SYNZIP2 (residues 23-29):SYNZIP1 (residues 23-29) are shown in cross-section, as viewed from the N-terminus. A partially buried water molecule is represented in purple. Crystal structure figures generated using PyMOL (DeLano Scientific, Palo Alto, CA). Helical wheel diagrams created using DrawCoil 1.0. (http://www.gevorggrigoryan.com/drawcoil/)

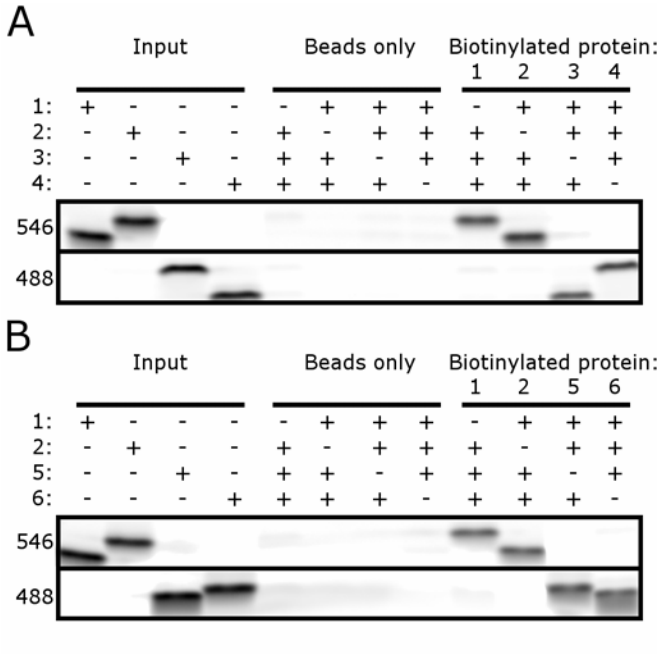

Figure 4. Biotin pull-down assay demonstrating specific interactions in each orthogonal set. (A, B) SYNZIPs 1 and 2 were labeled with Alexa Fluor 546 and SYNZIPS 3, 4, 5, and 6 were labeled with Alexa Fluor 488. Input lanes show each protein run individually. The beads-only lanes shows mixtures of the indicated fluorescent proteins incubated with NeutrAvidin beads. The biotinylated-protein lanes show mixtures of the 3 indicated fluorescent proteins (4 μM each) mixed with the indicated biotinylated protein at 4 μM, then incubated with NeutrAvidin beads. The two fluorescent channels 546 nm (top) and 488 nm (bottom) are indicated. (A) SYNZIP pairs 1-2 and 3-4. (B) SYNZIP pairs 1-2 and 5-6.

TOC:

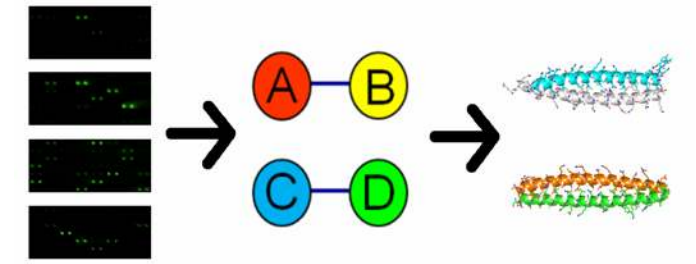

Supplementary Material for

A synthetic coiled-coil interactome provides heterospecific modules for molecular engineering

Aaron W. Reinke, Robert A. Grant and Amy E. Keating

MIT Department of Biology

77 Massachusetts Avenue

Cambridge, MA 02139

keating@mit.edu

A

```
SYNZIP peptides
SYNZIP1*   NLVAQLENEVASLENENETLKKKNLHKKDLIAYLEKEIANLRKKIEE
SYNZIP2*   ARNAYLRKKIARLKKDNLQLERDEQNLEKIIANLRDEIARLENEVASHEQ
SYNZIP3*   NEVTTLENDAAFIENENAYLEKEIARLRKEKAALRNRLAHKK
SYNZIP4*   QKVAELKNRVAVKLNRNEQLKNKVEELKNRNAYLKNELATLENEVARLENDVAE
SYNZIP5*   NTVKELKNYIQELEERNAELKNLKEHLKFAKAELEFELAAHKFE
SYNZIP6*   QKVAQLKNRVAYKLKENAKLENIVARLENDNANLEKDIANLEKDIANLERDVAR
SYNZIP7*   KEIEYLEKEIERLKDLREHLKQDNAAHRQELNALRLEEAKLEFILAHLLST
SYNZIP8*   KEIANLEKEIASLEKKVAVLKQRNAAHKQEVAALRKEIAYVEDEIQYVEDE
SYNZIP9*   QKVESLKQKIEELKQRKAQLKNDIANLEKEIAYAET
SYNZIP10*  NLLATLRSTAAVLENENHVLEKEKEKLRKEKEQLLNKLEAYK
SYNZIP11*  ELTDELKNKKEALRKDNAALLNELASLENEIANLEKEIAYFK
SYNZIP12*  NEDLVLENRLAALRNENAALENDLARLEKEIAYLEKEIEREK
SYNZIP13*  QKVEELKNKIAELENRNAVKKNRVAHLKQEIAYLKDELAAHEFE
SYNZIP14*  NDLDAYEREAEKLEKKNEVLRNRLAALENELATLRQEVASMKQELQS
SYNZIP15*  FENVTHEFILATLENENAKLRRLEAKLERELARLRNEVAWL
SYNZIP16*  NILASLENKKEELKKLNAHLLKEIENLEKEIANLEKEIAYFK
SYNZIP17*  NEKEELKSKKAELRNRIEQLKQKREQLKQKIANLRKEIEAYK
SYNZIP18*  SIAATLENDLARLENENARLEKDIANLERDLAKLEREEAYF
SYNZIP19*  NELESLENKKEELKNRNEELKQKREQLKQKLAALRNKLDAYKNRL
SYNZIP20*  STVEELLRAIQELEKRNAELKNRKEELKNLVAHLRQELAAHKYE
SYNZIP21*  NEVAQLENDVAVIENENAYLEKEIARLRKEIAALRDRLAHKK
SYNZIP22*  KRIAYLRKKIAALKKDNANLEKDIANLENEIERLIKEIKTLENEVASHEQ
SYNZIP23*  ALRAELKAKIALLRADNWALKRKAKDLRRLLRRLRNKAEELK
SYNZIP24   QKLQTLRDLLAVLENRNQELKQLRQHLKDLLKYLEDELATLEKE
SYNZIP25   NETEQLINKKEQLKNDNAALEKDAASLEKEIANLEKEIAYFK
SYNZIP26   EKIQELKRRLAYFRRENATLKNDNATLENELASVEAENEALRK
SYNZIP27   QKIQYLKQRIAELRKKIANLRKDIANLEDDAAVKEDELVHL
SYNZIP28   EKIEYLKDRIAELRSKIAALRNDLTHLKNDKAHKENELAHLA
SYNZIP29   NDIENLKDKIEELKQRKEELKQKIEYLKQKIEALRQKLAALKQRIA
SYNZIP30   EKIEELKDKIAELRSRNAALRNKIEALKQKLEALRQKIEYLKDRIA
SYNZIP31   AENQYVEDLIQYLEKENARLKKEVQRLVRELSYFRRRIAELA
SYNZIP32   AENQSVEDIIAKKEDENAHLKNEVKTLINELETLRKKIEYLA
SYNZIP33   RDLQNVEREIQSLEKKNESLKKKIASLENELATLKQEIAYFKRELAY
SYNZIP34   DRLAVKENRVAVLKNENAKLRNIIANLKDRIAYFRRELAYLELEEEQLA
SYNZIP35   NKVEQLKNKVEQLKNRNAALKNDLARLEREIAYAEE
SYNZIP36   EKNQELKNRLAVLENDNAALRNDLARLEREIAYME
SYNZIP37   KDIANLKKEIAHLKNDLQRLESIRERLKFDILNHEQEEYALE
SYNZIP38   NKNETLKNINARLRNDVARLKNRIARLKDDIENVEDEIQYLE
SYNZIP39   LENAQIKKEIAQLRKEVAQLKQKIEELKNDNARVEREIQYLE
SYNZIP40   QKRQQLKQKLAALRRDIENLQDEIAYKEDEIANLKDKIEQLLS
SYNZIP41   QKIESLKDKLANKRDKIALLRSEVASFEKEIAYLEKEIANLEN
SYNZIP42   EKIEYLKDKLAHKRNEVAQLRKEVTHKVDELTSLENEVAQLLK
SYNZIP43   QKVEQLKNKVEQKLKENESLENKVAELKNRNEYLKNKIENLINDITNLENDVAR
SYNZIP44   QKVAQLKNIIAKKEDENAVLENLVAVLENENAYLEKELARLERDIARAERDVKV
SYNZIP45   NRLQELENKNEVLEKRKAELRNEVATLEQELAAHRYELAAIEKEIA
SYNZIP46   KEIERLEKEIKTLINLLTTLRQDNAAHRKEAAALEKEEANLERDIQNLLRY
SYNZIP47   SKYDALRNKLEALKNRNAQLRKENEQLRLEEAVLEVRNEVL
SYNZIP48   QKIAYLRDRIAALKAENEALRAKNEALRSKIEELKKEKEELRDKIAQKKDR

Human peptides
BATF*      QKADTLHLESEDLEKQNAALRKEIKQLTEELKYFTSVLNSHE
FOS*       ELTDTLQAETDQLEDEKSALQTEIANLLKEKEKLEFILAAHR
ATF4*      AEQEALTGECKELEKKNEALKERADSLAKEIQYLKDLIEEVRKARGKKRV
ATF3       EKTECLQKESEKLESVNAELKAQIEELKNEKQHLIYMLNLHR
BACH1      DCIQNLESEIEKLQSEKESLLKERDHILSTLGETKQNLTGL
JUND       ERISRLEEKVKTLKSQNTELASTASLLREQVAQLKQKVLSHV
NFE2L3     DIILNLEDDVCNLQAKKETLKREQAQCNKAINIMKQKLHDL
Heptad     fgabcdefgabcdefgabcdefgabcdefgabcdefgabcdefgabcdefgabc
```

B

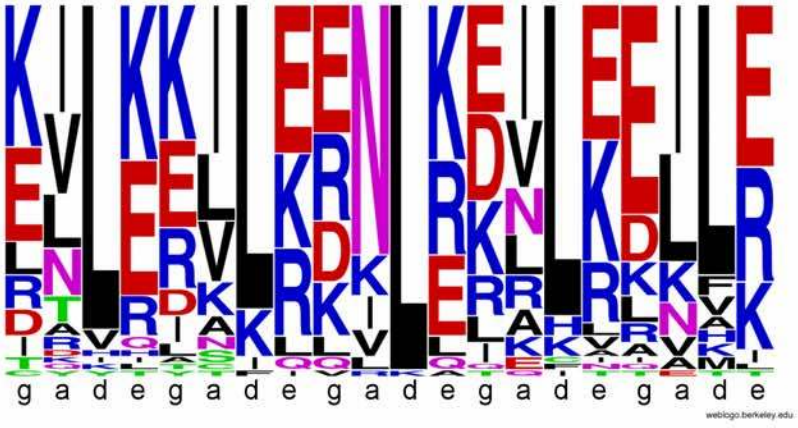

Figure S1. Sequences and sequence features of the 55 peptides measured. (A) Multiple-sequence alignment of the coiled-coil regions of the 55 peptides. Sequences start at an **f** position. Positions are colored as follows: **b**, **c,** and **f** positions (black), **g** (orange), **a** (blue), **d** (green), and **e** (purple). Peptides that form at least one hetero-specific interaction are indicated with an asterisk. (B) Sequence logo constructed using **a**, **d**, **e**, and **g** positions of the first 5 heptads of each peptide. See reference 1 for details. Sequence logo created with http://weblogo.berkeley.edu/[2].

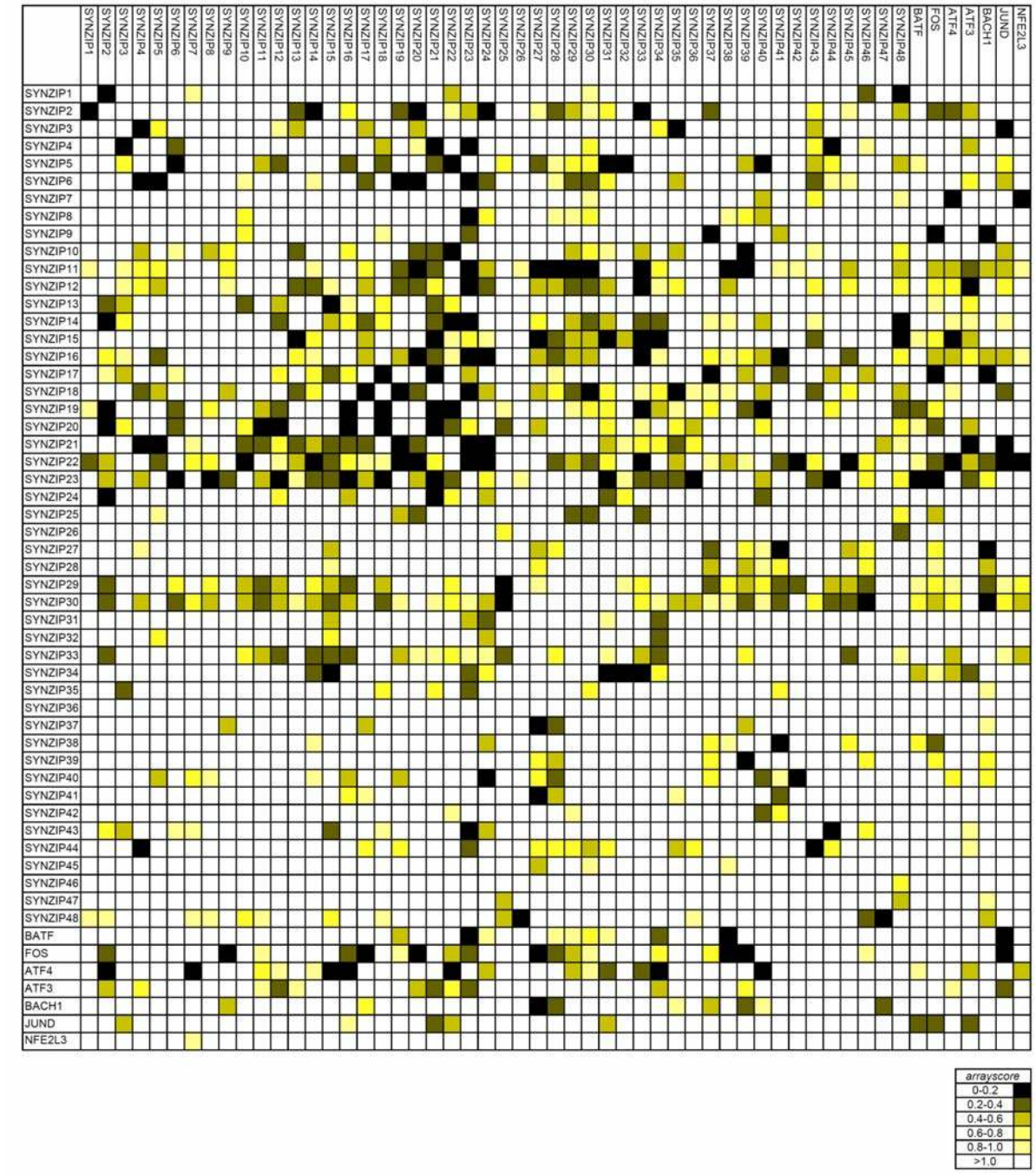

Figure S2. Array measurements for all 55 peptides. Peptides printed on the surface are listed in rows, and fluorescently labeled peptides in solution are listed in columns. Color indicates the strength of the array fluorescence signal, given as *arrayscore* values (see Methods) according to the color bar with 0 (black) indicating the strongest signal and >1 (white) indicating the weakest.

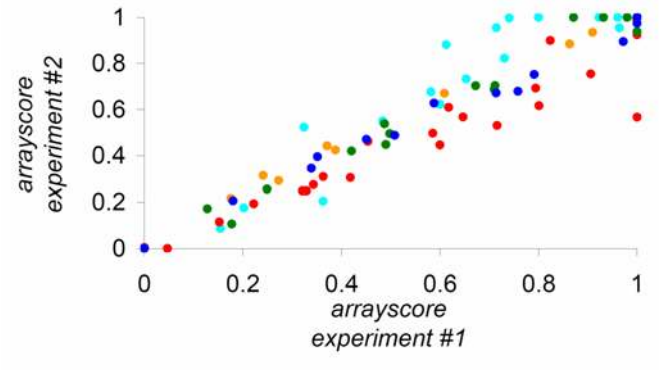

Figure S3. Reproducibility of the array experiments. Five solution probes measured in separate experiments are shown as a scatter plot. *Arrayscore* values >1 are set to 1. Blue, SYNZIP5 (R^2=.99). Orange, SYNZIP6 (R^2=.99). Teal, SYNZIP37 (R^2=.91). Red, FOS (R^2=.95). Green, ATF4 (R^2=.99).

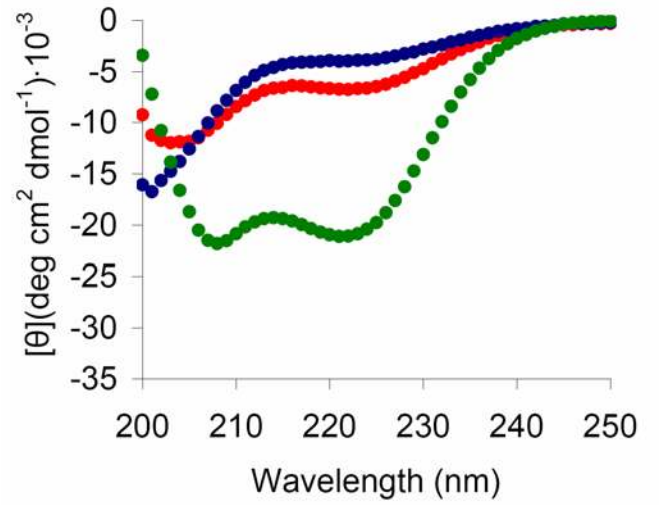

Figure S4. CD spectra for heterospecific pair SYNZIP6 + SYNZIP5. The mixture of SYNZIP5 with SYNZIP6 (4 μM each peptide) is in green**.** SYNZIP6 alone (4 μM) is in blue, SYNZIP5 alone (4 μM) is in red.

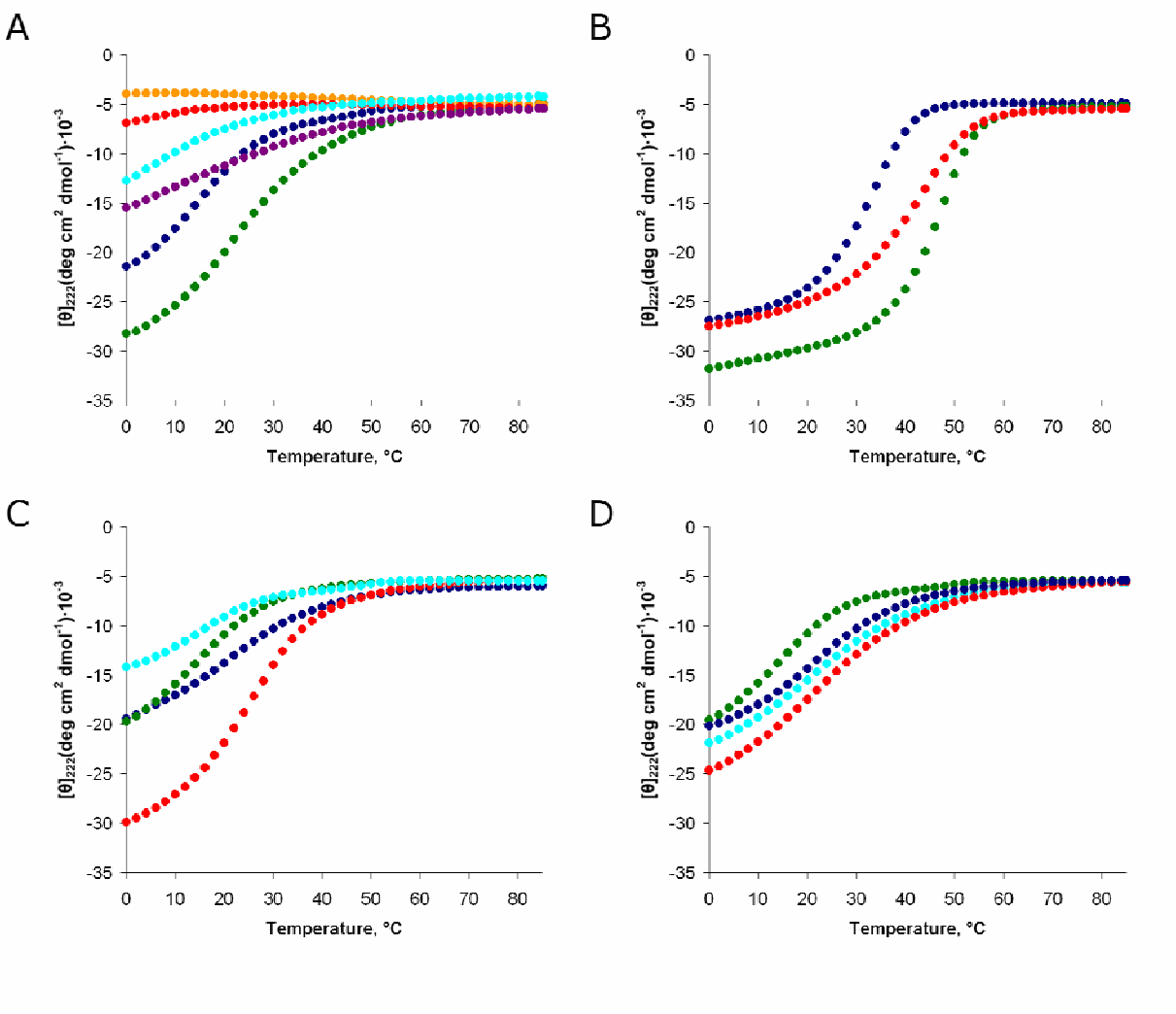

Figure S5. CD-monitored thermal melts of peptide pairs that form orthogonal sets. (A) Isolated peptides. ATF4-2 (green), SYNZIP1 (blue), SYNZIP3 (purple), SYNZIP5 (teal), SYNZIP4 (red), and SYNZIP6 (orange). (B) Interacting complexes**:** SYNZIP2 + SYNZIP1 (green), SYNZIP4 + SYNZIP3 (red), SYNZIP6 + SYNZIP5 (blue). (C) Non-interactions for orthogonal pair [SYNZIP2:SYNZIP1, SYNZIP6:SYNZIP5]: SYNZIP2 + SYNZIP5 (red), SYNZIP2 + SYNZIP6 (blue), SYNZIP1 + SYNZIP5 (green) + SYNZIP1 + SYNZIP6 (teal). (D) Non-interactions for orthogonal pair [SYNZIP2:SYNZIP1, SYNZIP4:SYNZIP3]: SYNZIP2 + SYNZIP3 (red), SYNZIP2 + SYNZIP4 (blue), SYNZIP1 + SYNZIP3 (teal) + SYNZIP1 + SYNZIP4 (green). Each individual peptide concentration was 4 μM, or 4 μM each (8 μM total peptide concentration) for mixtures.

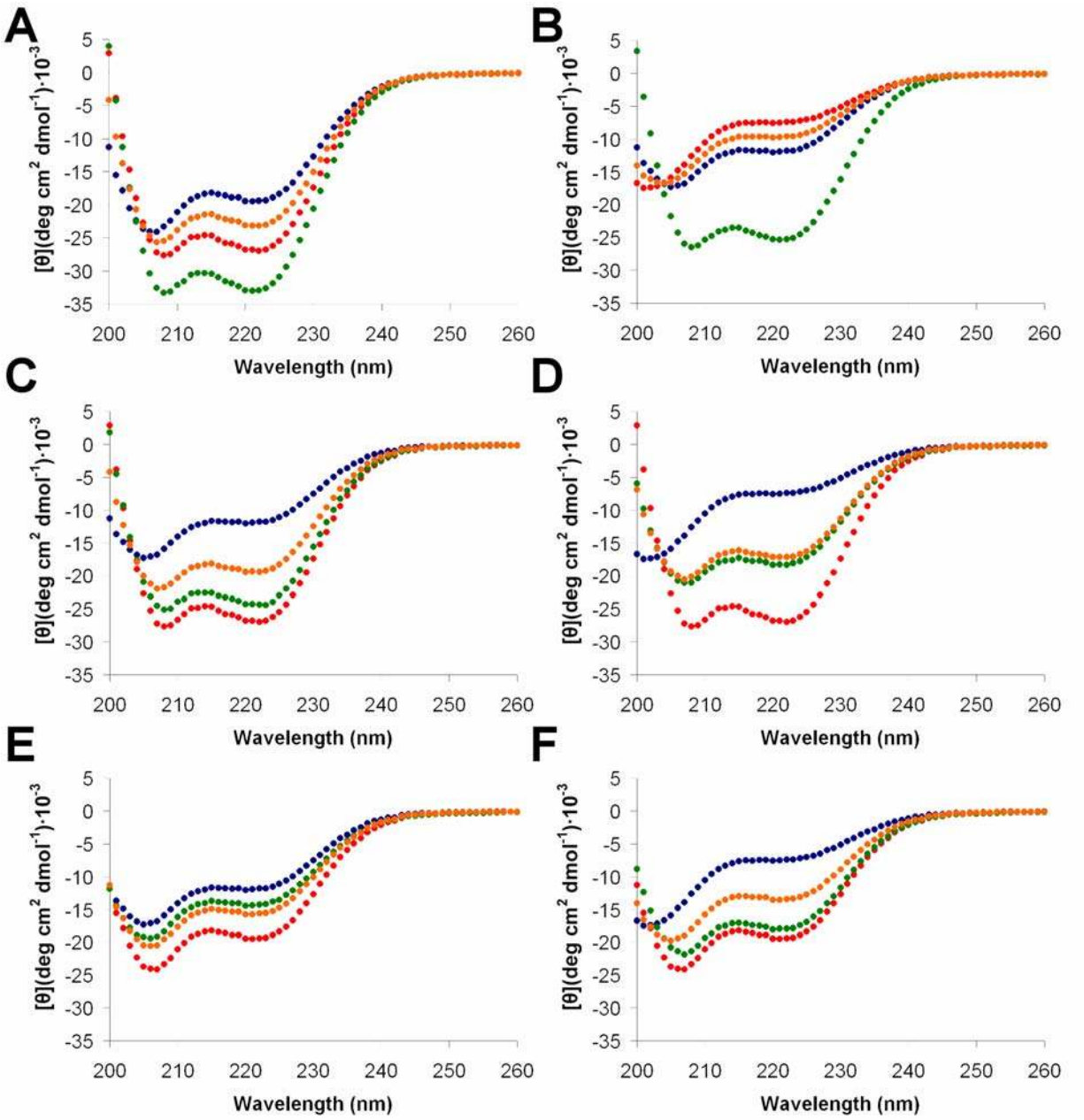

Figure S6. CD spectra characterizing an orthogonal set consisting of FOS:SYNZIP9 and SYNZIP3:SYNZIP4. (A, B) Characterization of 'on' interactions. (C-F) Characterization of 'off' interactions. (A) FOS (blue), SYNZIP9 (red), mixture of FOS + SYNZIP9 (green), and the mathematical average of the individual spectra (orange). (B) SYNZIP3 (blue), SYNZIP4 (red), mixture of SYNZIP3 + SYNZIP4 (green), and the average of the individual spectra (orange). (C) SYNZIP3 (blue), SYNZIP9 (red), mixture of SYNZIP3 + SYNZIP9 (green), and the average of the individual spectra (orange). (D) SYNZIP4 (blue), SYNZIP9 (red), mixture of SYNZIP4 + SYNZIP9 (green), and average of the individual spectra (orange). (E) SYNZIP3 (blue), FOS (red), mixture of SYNZIP3 + FOS (green), and average of the individual spectra (orange). (F) SYNZIP4 (blue), FOS (red), mixture of SYNZIP4 + FOS (green), and average of the individual spectra (orange). Spectra were measured at 25 °C at peptide concentrations of 40 µM or 20 µM of each peptide in mixtures (40 µM total peptide concentration).

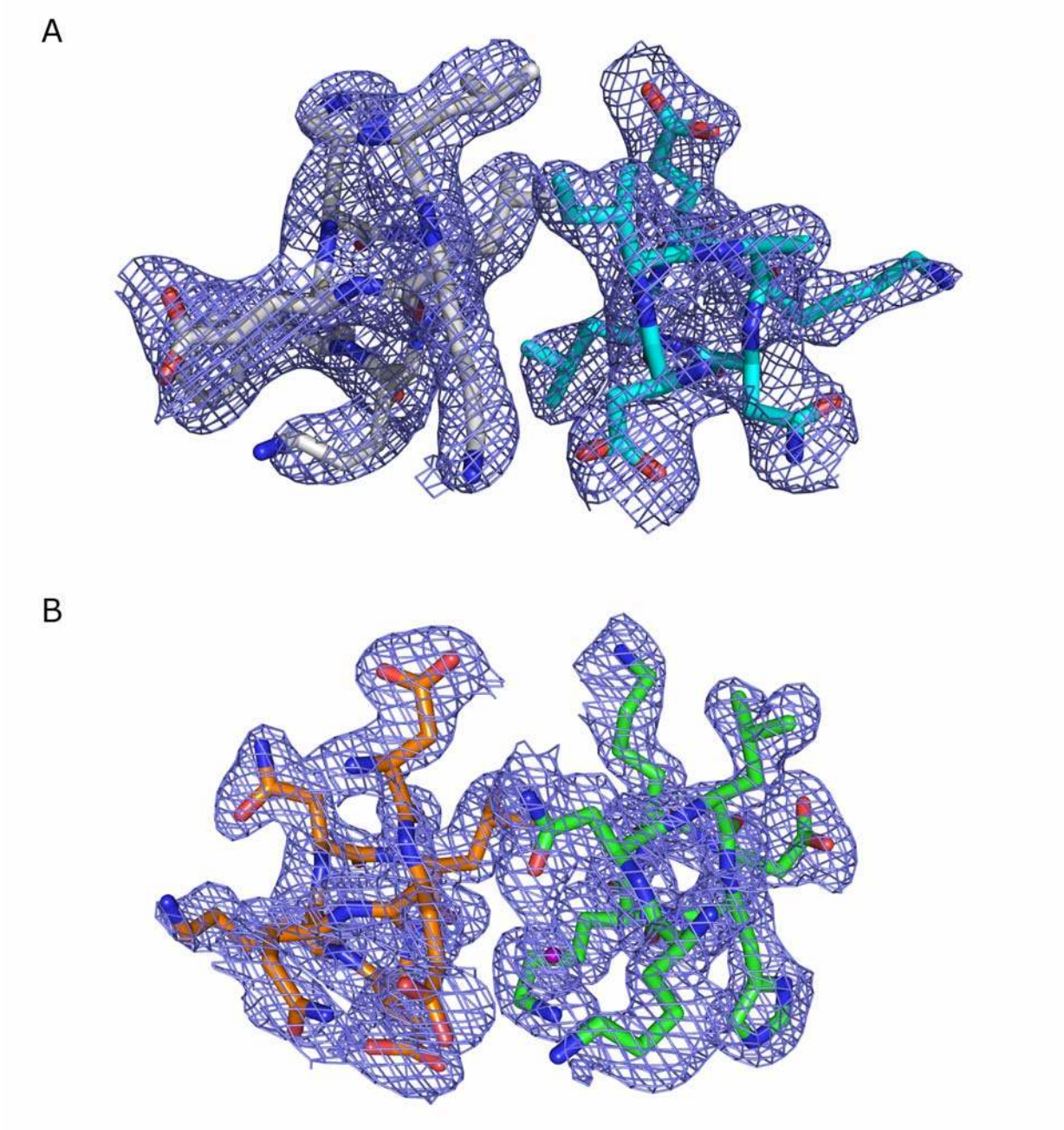

Figure S7. Electron density maps of SYNZIP5:SYNZIP6 and SYNZIP2:SYNZIP1. (A) The fourth heptad of SYNZIP5 (residues 23-29):SYNZIP6 (residues 37-43). (B) The fourth heptad of SYNZIP2 (residues 23-29):SYNZIP1(residues 23-29). These correspond to the heptads shown in Figure 3 G and H.

Table S1. Protein and DNA sequences used in this study.

Table S2. Average background-corrected fluorescence values from the array experiment.

Table S3. List of the proteins composing each of the subnetworks identified.

Table S4. Crystallographic data collection and refinement statistics.

Supplementary References

1. Grigoryan, G.; Reinke, A. W.; Keating, A. E. *Nature* **2009,** *458*, 859-864.
2. Crooks, G. E.; Hon, G.; Chandonia, J.-M.; Brenner, S. E. *Genome Research* **2004,** *14*, 1188-1190.

A synthetic coiled-coil interactome provides heterospecific modules for molecular engineering

A.W. Reinke, R.A. Grant & A.E. Keating

Table S1. Protein and DNA sequences used in this study.

Proteins used in array assay.

Name	Protein	DNA[e]	Source
SYNZIP1[a]	SYYHHHHHHLESTSLYKKAGSGSNLVAQLENEVASLEN ENETLKKKNLHKKDLIAYLEKEIANLRKKIEE	GGATCCAACCTGGTTGCGCAGCTCGAAAACGAAGTTGCGTCTCTGGAAAATGAGAACGA AACCCTGAAGAAAAAGAACCTGCACAAAAAAGACCTGATCGCGTACCTGGAGAAAGAAAT CGCGAATCTGCGTAAGAAAATCGAAGAATGATAACTCGAG	1
SYNZIP2[a]	SYYHHHHHHLESTSLYKKAGSGSARNAYLRKKIARLKKD NLQLERDEQNLEKIIANLRDEIARLENEVASHEQ	GGATCCGCGCGTAACGCGTATCTGCGTAAGAAAATCGCACGTCTGAAAAAAGACAACCT GCAGCTGGAACGTGATGAACAGAACCTGGAAAAAATCATCGCGAACCTGCGTGACGAAA TCGCGCGTCTCGAAAACGAAGTTGCGTCTCACGAACAGTGATAACTCGAG	1
SYNZIP3[a]	SYYHHHHHHLESTSLYKKAGSGSNEVTTLENDAAFIENE NAYLEKEIARLRKEKAALRNRLAHKK	GGATCCAACGAAGTTACCACTCTGGAGAATGACGCTGCGTTCATCGAAAATGAAAACGCT TACCTGGAAAAAGAAATCGCGCGTCTGCGTAAAGAAAAAGCGGCGCTGCGCAACCGTCT GGCGCACAAAAAATGATAACTCGAG	This study
SYNZIP4[a]	SYYHHHHHHLESTSLYKKAGSGSQKVAELKNRVAVKLN RNEQLKNKVEELKNRNAYLKNELATLENEVARLENDVAE	GGATCCCAGAAAGTTGCGGAACTCAAAAACCGTGTTGCGGTTAAACTGAATCGTAACGAA CAGCTGAAAAACAAAGTTGAAGAGCTGAAGAACCGTAACGCTTACCTCAAGAACGAACTG GCGACCCTGGAGAACGAGGTTGCGCGTCTGGAAAACGACGTTGCAGAATGATAACTCGA G	1
SYNZIP5[a]	SYYHHHHHHLESTSLYKKAGSGSNTVKELKNYIQELEER NAELKNLKEHLKFAKAELEFELAAHKFE	GGATCCAACACCGTTAAAGAACTGAAAAACTACATCCAGGAGCTGGAAGAGCGTAACGC TGAACTCAAAAACCTGAAGGAACACCTGAAATTCGCAAAAGCGGAACTGGAATTCGAACT GGCGGCTCACAAATTCGAGTGATAACTCGAG	1
SYNZIP6[a]	SYYHHHHHHLESTSLYKKAGSGSQKVAQLKNRVAYKLK ENAKLENIVARLENDNANLEKDIANLEKDIANLERDVAR	GGATCCCAAAAAGTTGCGCAGCTGAAAAACCGTGTTGCGTACAAACTGAAAGAAAACGC GAAGCTGGAGAACATCGTGGCGCGTCTGGAAAACGACAATGCGAACCTGGAGAAAGACA TTGCGAATCTCGAAAAGGACATCGCAAATCTGGAACGTGACGTTGCGCGTTGATAACTCG AG	1
SYNZIP7[a]	SYYHHHHHHLESTSLYKKAGSGSKEIEYLEKEIERLKDLR EHLKQDNAAHRQELNALRLEEAKLEFILAHLLST	GGATCCAAAGAGATCGAATACCTGGAAAAAGAAATTGAACGTCTGAAAGACCTGCGTGAA CACCTGAAACAGGACAACGCGGCTCACCGTCAGGAACTGAACGCGCTGCGTCTGGAAGA AGCGAAACTGGAATTCATCCTGGCGCACCTGCTGTCTACCTGATAACTCGAG	1
SYNZIP8[a]	SYYHHHHHHLESTSLYKKAGSGSKEIANLEKEIASLEKKV AVLKQRNAAHKQEVAALRKEIAYVEDEIQYVEDE	GGATCCAAAGAGATCGCTAACCTGGAGAAAGAAATTGCGTCTCTGGAAAAAAAGGTTGC GGTTCTGAAACAGCGTAACGCTGCGCACAAACAGGAAGTTGCGGCTCTGCGTAAGGAAA TCGCTTACGTGGAGGACGAAATCCAGTACGTTGAAGACGAATGATAACTCGAG	1
SYNZIP9[a]	SYYHHHHHHLESTSLYKKAGSGSQKVESLKQKIEELKQR KAQLKNDIANLEKEIAYAET	GGATCCCAGAAGGTTGAATCTCTGAAACAGAAAATCGAAGAACTGAAGCAGCGTAAAGC GCAGCTGAAAAACGACATCGCGAACCTGGAAAAAGAAATCGCGTATGCGGAAACCTGAT AACTCGAG	1
SYNZIP10[a]	SYYHHHHHHLESTSLYKKAGSGSNLLATLRSTAAVLENE NHVLEKEKEKLRKEKEQLLNKLEAYK	GGATCCAACCTGCTGGCGACCCTGCGTTCTACCGCTGCGGTTCTGGAAAACGAAAACCA CGTACTGGAGAAGGAGAAAGAGAAACTGCGCAAAGAAAAAGAACAGCTGCTGAACAAAC TGGAAGCGTACAAATGATAACTCGAG	This study
SYNZIP11[a]	SYYHHHHHHLESTSLYKKAGSGSELTDELKNKKEALRK DNAALLNELASLENEIANLEKEIAYFK	GGATCCGAACTGACCGATGAACTGAAAAACAAAAAAGAAGCTCTGCGTAAAGACAACGCT GCGCTGCTGAACGAACTGGCGTCTCTGGAAAACGAAATTGCGAACCTGGAGAAAGAAAT CGCGTACTTCAAATGATAACTCGAG	1
SYNZIP12[a]	SYYHHHHHHLESTSLYKKAGSGSNEDLVLENRLAALRN ENAALENDLARLEKEIAYLEKEIEREK	GGATCCAATGAAGACCTGGTTCTGGAAAACCGCCTTGCGGCGCTGCGTAACGAAAACGC TGCGCTTGAGAATGACCTGGCGCGTCTGGAGAAAGAGATCGCGTACTTGGAGAAGGAAA TCGAACGTGAAAAATGATAACTCGAG	This study
SYNZIP13[a]	SYYHHHHHHLESTSLYKKAGSGSQKVEELKNKIAELENR NAVKKNRVAHLKQEIAYLKDELAAHEFE	GGATCCCAGAAAGTTGAAGAACTGAAAAACAAAATCGCGGAACTGGAAAACCGTAACGC GGTTAAAAAGAACCGTGTTGCGCACCTGAAACAGGAAATCGCTTATCTGAAAGACGAACT GGCGGCTCACGAATTTGAATGATAACTCGAG	1
SYNZIP14[a]	SYYHHHHHHLESTSLYKKAGSGSNDLDAYEREAEKLEK KNEVLRNRLAALENELATLRQEVASMKQELQS	GGATCCAACGACCTGGACGCGTACGAACGTGAAGCGGAAAAACTGGAAAAGAAAAACGA AGTTCTGCGTAACCGTCTGGCGGCTCTCGAAAACGAGCTGGCGACCCTGCGTCAGGAAG TTGCGTCTATGAAACAGGAACTGCAATCTTGATAACTCGAG	1
SYNZIP15[a]	SYYHHHHHHLESTSLYKKAGSGSFENVTHEFILATLENE NAKLRRLEAKLERELARLRNEVAWL	GGATCCTTTGAAAACGTTACCCACGAATTCATCCTGGCGACCCTGGAAAACGAAAACGCT AAACTGCGTCGTCTGGAAGCGAAACTGGAACGTGAACTGGCTCGTCTGCGTAACGAAGT TGCGTGGCTGTGATAACTCGAG	1
SYNZIP16[a]	SYYHHHHHHLESTSLYKKAGSGSNILASLENKKEELKKL NAHLLKEIENLEKEIANLEKEIAYFK	GGATCCAACATCCTGGCGTCTCTCGAAAACAAAAAAGAAGAACTGAAAAAACTGAACGCG CACCTGCTGAAAGAAATCGAAAATCTGGAGAAAGAGATCGCAAACCTGGAAAAGGAAATC GCGTACTTCAAATGATAACTCGAG	1
SYNZIP17[a]	SYYHHHHHHLESTSLYKKAGSGSNEKEELKSKKAELRN RIEQLKQKREQLKQKIANLRKEIEAYK	GGATCCAACGAAAAAGAAGAACTGAAATCCAAAAAAGCGGAACTGCGCAACCGTATCGA ACAGCTGAAACAGAAACGTGAACAACTGAAGCAGAAAATCGCGAACCTGCGTAAAGAAAT CGAAGCTTACAAATGATAACTCGAG	1
SYNZIP18[a]	SYYHHHHHHLESTSLYKKAGSGSSIAATLENDLARLENE NARLEKDIANLERDLAKLEREEAYF	GGATCCAGCATCGCGGCGACCCTGGAGAACGATCTGGCGCGTCTGGAAAACGAAAACG CTCGTCTCGAAAAAGACATCGCGAACCTGGAACGTGACCTGGCGAAACTGGAGCGTGAA GAAGCGTACTTCTGATAACTCGAG	1
SYNZIP19[a]	SYYHHHHHHLESTSLYKKAGSGSNELESLENKKEELKN RNEELKQKREQLKQKLAALRNKLDAYKNRL	GGATCCAACGAACTGGAATCTCTGGAGAACAAAAAAGAAGAACTGAAGAACCGTAACGA AGAGCTGAAGCAGAAACGTGAACAGCTGAAACAGAAACTGGCGGCTCTGCGTAACAAAC TGGACGCGTACAAAAACCGTCTGTGATAACTCGAG	1
SYNZIP20[a]	SYYHHHHHHLESTSLYKKAGSGSSTVEELLRAIQELEKR NAELKNRKEELKNLVAHLRQELAAHKYE	GGATCCAGCACTGTTGAAGAACTGCTGCGTGCGATCCAGGAGCTGGAAAAACGTAACGC GGAACTCAAAAACCGTAAAGAGGAACTGAAAAATCTGGTTGCGCACCTGCGTCAAGAGC TGGCAGCGCACAAATACGAATGATAACTCGAG	1
SYNZIP21[a]	SYYHHHHHHLESTSLYKKAGSGSNEVAQLENDVAVIEN ENAYLEKEIARLRKEIAALRDRLAHKK	GGATCCAACGAAGTTGCGCAGCTGGAAAACGACGTTGCGGTTATCGAAAATGAAAACGC GTACCTGGAGAAGGAGATCGCGCGTCTGCGTAAAGAAATTGCGGCGCTGCGTGACCGTC TGGCGCACAAAAAATGATAACTCGAG	This study
SYNZIP22[a]	SYYHHHHHHLESTSLYKKAGSGSKRIAYLRKKIAALKKD NANLEKDIANLENEIERLIKEIKTLENEVASHEQ	GGATCCAAACGTATCGCGTACCTGCGTAAGAAAATCGCGGCACTGAAAAAAGACAACGC GAACCTCGAAAAAGATATCGCAAACCTGGAAAACGAAATCGAACGTCTGATCAAAGAAAT CAAAACCCTGGAGAACGAAGTTGCGTCTCACGAACAGTGATAACTCGAG	1
SYNZIP23[a]	SYYHHHHHHLESTSLYKKAGSGSALRAELKAKIALLRAD NWALKRKAKDLRRLLRRLRNKAEELK	GGATCCGCACTCCGTGCGGAACTGAAAGCGAAAATCGCGCTCCTGCGTGCTGACAACTG GGCGCTGAAACGTAAAGCTAAAGACCTGCGTCGTCTGCTGCGCCGTCTGCGTAACAAAG CGGAAGAGCTGAAATGATAACTCGAG	This study
SYNZIP24[a]	SYYHHHHHHLESTSLYKKAGSGSQKLQTLRDLLAVLENR NQELKQLRQHLKDLLKYLEDELATLEKE	GGATCCCAGAAACTGCAGACCCTGCGTGATCTGCTGGCGGTTCTGGAGAACCGTAATCA GGAACTGAAACAGCTGCGTCAGCACCTGAAAGACCTGCTGAAATACCTGGAAGACGAAC TGGCGACCCTGGAAAAAGAATGATAACTCGAG	1
SYNZIP25[a]	SYYHHHHHHLESTSLYKKAGSGSNETEQLINKKEQLKND NAALEKDAASLEKEIANLEKEIAYFK	GGATCCAACGAAACCGAACAGCTGATCAACAAAAAAGAGCAGCTGAAAAACGACAACGC AGCGCTCGAAAAAGATGCGGCGTCTCTGGAAAAGGAAATCGCGAACCTGGAGAAAGAAA TTGCGTACTTCAAATGATAACTCGAG	1
SYNZIP26[a]	SYYHHHHHHLESTSLYKKAGSGSEKIQELKRRLAYFRRE NATLKNDNATLENELASVEAENEALRK	GGATCCGAAAAAATCCAGGAACTGAAACGTCGTCTGGCGTACTTCCGTCGTGAAAACGC GACCCTGAAAAACGACAACGCTACCCTGGAGAACGAACTGGCGTCTGTTGAAGCGGAAA ACGAAGCGCTGCGTAAATGATAACTCGAG	1

SYNZIP27[a]	SYYHHHHHHLESTSLYKKAGSGSQKIQYLKQRIAELRKKIANLRKDIANLEDDAAVKEDELVHL	GGATCCCAGAAAATCCAGTACCTGAAACAGCGTATCGCGGAACTGCGTAAAAAGATTGCGAACCTGCGCAAAGACATCGCTAACCTGGAAGATGACGCTGCGGTTAAAGAAGACGAACTGGTTCACCTGTGATAACTCGAG	1
SYNZIP28[a]	SYYHHHHHHLESTSLYKKAGSGSEKIEYLKDRIAELRSKIAALRNDLTHLKNDKAHKENELAHLA	GGATCCGAAAAAATCGAATACCTGAAAGACCGTATCGCGGAACTGCGTTCTAAAATCGCTGCGCTGCGTAACGACCTGACCCACCTGAAGAACGACAAAGCGCACAAAGAAAACGAACTGGCGCACCTGGCGTGATAACTCGAG	1
SYNZIP29[a]	SYYHHHHHHLESTSLYKKAGSGSNDIENLKDKIEELKQRKEELKQKIEYLKQKIEALRQKLAALKQRIA	GGATCCAACGACATCGAAAACCTGAAAGACAAGATCGAAGAACTCAAACAGCGTAAAGAAGAGCTGAAACAGAAAATCGAATACCTCAAGCAGAAGATTGAAGCGCTGCGTCAGAAACTGGCGGCTCTGAAGCAGCGTATCGCGTGATAACTCGAG	1
SYNZIP30[a]	SYYHHHHHHLESTSLYKKAGSGSEKIEELKDKIAELRSRNAALRNKIEALKQKLEALRQKIEYLKDRIA	GGATCCGAAAAAATCGAAGAACTGAAAGACAAAATCGCGGAACTGCGTTCTCGTAACGCTGCGCTGCGTAACAAAATTGAAGCGCTGAAACAGAAACTGGAAGCTCTGCGTCAGAAGATCGAATACCTCAAAGACCGTATCGCGTGATAACTCGAG	1
SYNZIP31[a]	SYYHHHHHHLESTSLYKKAGSGSAENQYVEDLIQYLEKENARLKKEVQRLVRELSYFRRRIAELA	GGATCCGCTGAAAACCAGTACGTTGAAGACCTGATCCAGTACCTGGAAAAAGAGAACGCTCGTCTGAAAAAAGAAGTTCAGCGTCTGGTTCGTGAACTGTCTTACTTCCGTCGTCGTATCGCGGAACTGGCGTGATAACTCGAG	1
SYNZIP32[a]	SYYHHHHHHLESTSLYKKAGSGSAENQSVEDIIAKKEDENAHLKNEVKTLINELETLRKKIEYLA	GGATCCGCTGAAAACCAGTCTGTTGAAGACATCATCGCGAAAAAAGAAGATGAAAACGCGCACCTGAAAAACGAAGTTAAAACCCTGATCAACGAACTGGAAACTCTGCGTAAGAAAATCGAATACCTGGCGTGATAACTCGAG	1
SYNZIP33[a]	SYYHHHHHHLESTSLYKKAGSGSRDLQNVEREIQSLEKKNESLKKKIASLENELATLKQEIAYFKRELAY	GGATCCCGTGACCTGCAGAACGTTGAACGTGAAATCCAGTCCCTGGAAAAGAAAAACGAATCTCTGAAGAAGAAAATCGCTTCTCTGGAGAACGAACTGGCGACCCTGAAACAGGAAATCGCGTACTTCAAACGTGAGCTGGCTTACTGATAACTCGAG	1
SYNZIP34[a]	SYYHHHHHHLESTSLYKKAGSGSDRLAVKENRVAVLKNENAKLRNIIANLKDRIAYFRRELAYLELEEEQLA	GGATCCGACCGTCTGGCGGTTAAAGAAAACCGTGTTGCGGTTCTGAAAAACGAAAACGCGAAACTGCGTAACATCATCGCGAACCTGAAAGACCGTATCGCGTACTTCCGTCGTGAACTGGCGTACCTGGAACTGGAAGAAGAACAGCTGGCGTGATAACTCGAG	1
SYNZIP35[a]	SYYHHHHHHLESTSLYKKAGSGSNKVEQLKNKVEQLKNRNAALKNDLARLEREIAYAEE	GGATCCAACAAGGTTGAGCAGCTCAAAAACAAAGTTGAACAGCTGAAAAACCGTAACGCTGCGCTGAAGAACGACCTGGCGCGTCTGGAACGTGAAATCGCGTATGCGGAAGAATGATAACTCGAG	1
SYNZIP36[a]	SYYHHHHHHLESTSLYKKAGSGSEKNQELKNRLAVLENDNAALRNDLARLEREIAYME	GGATCCGAAAAAAACCAGGAACTGAAAAACCGTCTGGCGGTTCTGGAAAACGACAACGCTGCTCTGCGTAACGACCTGGCGCGTCTGGAACGTGAAATCGCGTACATGGAATGATAACTCGAG	1
SYNZIP37[a]	SYYHHHHHHLESTSLYKKAGSGSKDIANLKKEIAHLKNDLQRLESIRERLKFDILNHEQEEYALE	GGATCCAAAGACATCGCGAACCTCAAAAAAGAAATCGCGCACCTGAAAAACGACCTGCAGCGTCTGGAATCTATCCGTGAACGTCTGAAATTCGACATTCTGAACCACGAACAGGAAGAATACGCACTGGAATGATAACTCGAG	1
SYNZIP38[a]	SYYHHHHHHLESTSLYKKAGSGSNKNETLKNINARLRNDVARLKNRIARLKDDIENVEDEIQYLE	GGATCCAACAAAAACGAAACTCTGAAGAACATCAACGCACGTCTGCGTAACGATGTTGCTCGTCTCAAAAACCGTATCGCGCGTCTGAAAGACGACATCGAAAACGTTGAAGACGAAATCCAGTACCTGGAATGATAACTCGAG	1
SYNZIP39[a]	SYYHHHHHHLESTSLYKKAGSGSLENAQIKKEIAQLRKEVAQLKQKIEELKNDNARVEREIQYLE	GGATCCCTGGAAAACGCTCAGATCAAAAAAGAAATCGCTCAGCTGCGTAAAGAAGTTGCACAGCTGAAACAGAAAATCGAAGAACTGAAAAACGATAACGCACGTGTTGAACGTGAAATCCAGTACCTGGAATGATAACTCGAG	1
SYNZIP40[a]	SYYHHHHHHLESTSLYKKAGSGSQKRQQLKQKLAALRRDIENLQDEIAYKEDEIANLKDKIEQLLS	GGATCCCAGAAACGTCAGCAACTGAAACAGAAACTGGCGGCTCTGCGTCGTGACATCGAAAACCTGCAAGATGAAATCGCGTACAAAGAAGACGAAATTGCGAACCTGAAAGACAAAATCGAACAGCTGCTGTCTTGATAACTCGAG	1
SYNZIP41[a]	SYYHHHHHHLESTSLYKKAGSGSQKIESLKDKLANKRDKIALLRSEVASFEKEIAYLEKEIANLEN	GGATCCCAGAAAATCGAATCTCTGAAAGACAAACTGGCGAACAAACGTGACAAAATCGCGCTGCTGCGTTCTGAAGTTGCGTCTTTTGAAAAAGAAATCGCATACCTGGAGAAAGAGATCGCAAACCTGGAAAACTGATAACTCGAG	1
SYNZIP42[a]	SYYHHHHHHLESTSLYKKAGSGSEKIEYLKDKLAHKRNEVAQLRKEVTHKVDELTSLENEVAQLLK	GGATCCGAAAAAATCGAATACCTGAAAGACAAACTGGCGCACAAACGTAACGAAGTTGCTCAGCTGCGTAAAGAAGTTACCCACAAAGTTGACGAACTGACCTCTCTGGAAAACGAGGTTGCACAGCTGCTGAAATGATAACTCGAG	1
SYNZIP43[a]	SYYHHHHHHLESTSLYKKAGSGSQKVEQLKNKVEQKLKENESLENKVAELKNRNEYLKNKIENLINDITNLENDVAR	GGATCCCAGAAAGTGGAACAGCTGAAGAACAAGGTTGAACAGAAACTGAAAGAGAACGAGTCTCTGGAGAACAAAGTTGCGGAGCTGAAAAACCGTAACGAGTACCTCAAAAACAAAATCGAGAACCTGATCAACGACATCACCAACCTGGAAAACGACGTTGCGCGTTGATAACTCGAG	1
SYNZIP44[a]	SYYHHHHHHLESTSLYKKAGSGSQKVAQLKNIIAKKEDENAVLENLVAVLENENAYLEKELARLERDIARAERDVKV	GGATCCCAGAAAGTTGCGCAGCTGAAAAACATCATCGCGAAAAAAGAAGATGAGAACGCTGTTCTGGAAAACCTGGTTGCGGTGCTGGAGAACGAAAACGCGTACCTCGAAAAGGAACTGGCGCGTCTGGAACGCGACATCGCGCGTGCGGAACGTGATGTTAAAGTTTGATAACTCGAG	1
SYNZIP45[a]	SYYHHHHHHLESTSLYKKAGSGSNRLQELENKNEVLEKRKAELRNEVATLEQELAAHRYELAAIEKEIA	GGATCCAACCGTCTGCAGGAACTGGAAAACAAAAACGAGGTTCTGGAGAAACGTAAAGCGGAACTGCGCAACGAAGTTGCGACCCTGGAACAGGAGCTGGCTGCGCACCGTTACGAACTGGCGGCGATCGAAAAAGAAATCGCATGATAACTCGAG	1
SYNZIP46[a]	SYYHHHHHHLESTSLYKKAGSGSKEIERLEKEIKTLINLLTTLRQDNAAHRKEAAALEKEEANLERDIQNLLRY	GGATCCAAAGAAATCGAACGTCTGGAAAAAGAGATCAAAACCCTGATCAACCTCCTGACCACCCTGCGTCAGGACAACGCGGCACACCGTAAAGAAGCAGCGGCACTGGAGAAAGAAGAAGCGAACCTGGAACGTGACATCCAGAACCTGCTGCGTTACTGATAACTCGAG	1
SYNZIP47[a]	SYYHHHHHHLESTSLYKKAGSGSSKYDALRNKLEALKNRNAQLRKENEQLRLEEAVLEVRNEVL	GGATCCAGCAAATACGACGCGCTGCGTAACAAACTGGAAGCGCTGAAAAACCGTAACGCGCAGCTCCGTAAAGAAAACGAACAGCTGCGTCTGGAAGAAGCGGTTCTGGAGGTTCGTAACGAAGTTCTGTGATAACTCGAG	1
SYNZIP48[a]	SYYHHHHHHLESTSLYKKAGSGSQKIAYLRDRIAALKAENEALRAKNEALRSKIEELKKEKEELRDKIAQKKDR	GGATCCCAGAAAATTGCGTACCTGCGTGATCGTATCGCGGCACTGAAAGCTGAAAACGAAGCTCTGCGTGCGAAAAATGAAGCGCTGCGTTCTAAAATCGAGGAACTGAAGAAAGAAAAAGAAGAACTGCGCGACAAAATCGCTCAGAAAAAAGACCGTTGATAACTCGAG	1
BATF[b]	SYYHHHHHHLESTSLYKKAGSGSQKADTLHLESEDLEKQNAALRKEIKQLTEELKYFTSVLNSHELE		2
FOS[b]	SYYHHHHHHLESTSLYKKAGSEFFRRERNKMAAAKCRNRRRELTDTLQAETDQLEDEKSALQTEIANLLKEKEKLEFILAAHRPACKIPDDLGFPEEMSLE		2
ATF4[b]	SYYHHHHHHLESTSLYKKAGSEFNKTAATRYRQKKRAEQEALTGECKELEKKNEALKERADSLAKEIQYLKDLIEEVRKARGKKRVP		2
ATF3[b]	SYYHHHHHHLESTSLYKKAGSGSCPEEDERKKRRRERNKIAAAKCRNKKKEKTECLQKESEKLESVNAELKAQIEELKNEKQHLIYMLNLHRPTCIVRAQNGRTPEDLE		2
BACH1[b]	SYYHHHHHHLESTSLYKKAGSEFGCRKRKLDCIQNLESEIEKLQSEKESLLKERDHILSTLGETKQNLTGLCQKVCKEAALSQEQNLE		2

JUND[b]	SYYHHHHHHLESTSLYKKAGSGSERISRLEEKVKTLKSQNTELASTASLLREQVAQLKQKVLSHVLE		2
NFE2L3[b]	SYYHHHHHHLESTSLYKKAGSEFGDIRRRGKNKVAAQNCRKRKLDIILNLEDDVCNLQAKKETLKREQAQCNKAINIMKQKLHDLYHDIFSRLRDDQGRPVLE		2
Proteins used in circular dichroism and crystallography studies.			
SYNZIP1[c]	GSNLVAQLENEVASLENENETLKKKNLHKKDLIAYLEKEIANLRKKIEE		This study
SYNZIP2[c]	GSARNAYLRKKIARLKKDNLQLERDEQNLEKIIANLRDEIARLENEVASHEQ		This study
SYNZIP3[c]	GSNEVTTLENDAAFIENENAYLEKEIARLRKEKAALRNRLAHKK		This study
SYNZIP4[c]	GSQKVAELKNRVAVKLNRNEQLKNKVEELKNRNAYLKNELATLENEVARLENDVAE		This study
SYNZIP5[c]	GSNTVKELKNYIQELEERNAELKNLKEHLKFAKAELEFELAAHKFE		This study
SYNZIP6[c]	GSQKVAQLKNRVAYKLKENAKLENIVARLENDNANLEKDIANLEKDIANLERDVAR		This study
SYNZIP9[c]	GSQKVESLKQKIEELKQRKAQLKNDIANLEKEIAYAET		This study
FOS LZ[c]	GSELTDTLQAETDQLEDEKSALQTEIANLLKEKEKLEFILAAHR	GGATCCGAACTGACCGACACTCTGCAGGCGGAAACCGACCAGCTCGAAGATGAAAAATCTGCGCTGCAGACCGAAATCGCGAACCTGCTGAAAGAAAAAGAGAAACTGGAATTCATCCTGGCTGCTCACCGTTGATAACTCGAG	This study
SYNZIP4(1-42)[c]	GSQKVAELKNRVAVKLNRNEQLKNKVEELKNRNAYLKNELATLE		This study
SYNZIP4(15-54)[c]	GSNRNEQLKNKVEELKNRNAYLKNELATLENEVARLENDVAE		This study
Proteins used in pull-down assays.			
SYNZIP1(1-47)[d]	GSCGSNLVAQLENEVASLENENETLKKKNLHKKDLIAYLEKEIANLRKKIEE		This study
SYNZIP2(1-47)[d]	GSCGSARNAYLRKKIARLKKDNLQLERDEQNLEKIIANLRDEIARLENEVAS		This study
SYNZIP3(1-40)[d]	GSCGSNEVTTLENDAAFIENENAYLEKEIARLRKEKAALRNRLAH		This study
SYNZIP4(15-54)[d]	GSCGSNRNEQLKNKVEELKNRNAYLKNELATLENEVARLENDVAE		This study
SYNZIP5(1-40)[d]	GSCGSNTVKELKNYIQELEERNAELKNLKEHLKFAKAELEFELAA		This study
SYNZIP6(15-54)[d]	GSCGSKENAYLENIVARLENDNANLEKDIANLEKDIANLERDVAR		This study
[a] SYNZIP protein constructs used for array measurments have the following linker at the N-Terminus including the BamHI site: SYYHHHHHHLESTSLYKKAGSGS			
[b] The coiled-coil region of the human sequences is in green. Additional human protein sequence is in red. Cloning sequence is in black.			
[c] Constructs used for circular dichroism and crystallography studies include a GS at the N-Terminus after cleavage by TEV.			
[d] Constructs used in pull-down assays include a GS at the N-Terminus after cleavage by TEV and a cysteine followed by a short GS linker.			
[e] DNA sequence is of the insert and includes BamHI and XhoI sites that were used for cloning. DNA sequence for proteins used in array studies is the same for the proteins used in other assays unless otherwise indicated.			
References			
1	Grigoryan, G., Reinke, A. W. & Keating, A. E. Design of protein-interaction specificity gives selective bZIP-binding peptides. Nature 458, 859-864 (2009).		
2	Newman, J. R. S. & Keating, A. E. Comprehensive Identification of Human bZIP Interactions with Coiled-Coil Arrays. Science 300, 2097-2101 (2003).		

A synthetic coiled-coil interactome provides heterospecific modules for molecular engineering
"A.W. Reinke, R.A. Grant & A.E. Keating"
Table S2. Average background corrected values from the array experiment. Peptides in solution are in columns and those on the surface are in rows. Duplicates are indicated with a number 2 in parentheses.

Protein	SYNZIP1	SYNZIP2	SYNZIP3	SYNZIP4	SYNZIP5	SYNZIP6	SYNZIP7	SYNZIP8	SYNZIP9	SYNZIP10	SYNZIP11	SYNZIP12	SYNZIP13	SYNZIP14	SYNZIP15	SYNZIP16	SYNZIP17	SYNZIP18	SYNZIP19	SYNZIP20	SYNZIP21	SYNZIP22	SYNZIP23	SYN24	SYN25	SYN26	SYN27	SYN28	SYN29	SYN30	SYN31	SYN32	SYN33	SYN34	SYN35	SYN36	SYN37	SYN38	SYN39	SYN40	SYN41	SYN42	SYN43	SYN44	SYN45	SYN46	SYN47	SYN48	BATF	FOS	ATF4	ATF3	BACH1	JUND	NFE2L3	SYNZIP5(2)	SYN37(2)	SYNZIP6(2)	ATF4(2)	FOS(2)
SYNZIP1	2727	47850.75	605.875	1205.625	22.875	199.5	4675.375	299.5	38	-30.5	3129.375	208.875	674	460.625	1026	2663.5	1067.25	-239.75	5059.625	4305.75	1348.75	13166	11992.625	2089.125	571.375	741.875	985.25	392.375	2686.75	5131.875	1478.375	38.5	305.75	549.5	446.125	412.625	710.5	541.25	429.25	1523.125	999.125	432.625	134	23.875	620.75	14386	575.875	14520	-75.75	1417.375	3053.75	1420	1577.625	3627.125	2925.125	290.375	380.25	163.875	1997.25	1168.5
SYNZIP2	49531.5	4907.125	1023	1079.125	224.625	491	3565.875	3800.125	1065.625	-103.375	602.375	1427.125	17562.125	42445.5	-2040.375	16600.375	5490	306	24005.875	33929.25	7554.75	5972.25	20889.375	31406.75	114.25	581.125	8668.25	18089.25	8859.125	5370	16270.25	385.625	38042.5	2768	-40.875	139	16860.25	790.25	1660.375	1912.625	671.625	648.625	7749.125	-270.625	2049	2085.125	244	7664.75	1308	17359.625	28082.75	18064.75	1266.875	7929.5	1109.625	1068.25	7298.625	763	22237.25	18017.75
SYNZIP3	-484.375	1852.875	-583.25	34221.375	7000.875	99.375	-113.75	1257	467.875	-591.875	4448.75	6912.375	14412.75	6351.125	6177.375	11614.25	15054.125	-255.25	1281.875	16144	9319.25	1659.75	10970.75	2170.875	-27.875	243.875	170.625	12	1133	1757.5	9286.625	889.25	2402.25	9764.75	13850	3096.625	701.875	2401.125	617.75	-132.625	164.875	359.75	8791.125	-106.75	370.25	28.375	950	-123.625	447.75	-556.25	5823	3581	134.5	28656.25	-86.875	11407.375	-180	418	4817.25	-658.25
SYNZIP4	-314.75	2693.75	36766.875	-52.5	-8.25	15580.75	210.125	1145.5	-220.25	2395.375	489.625	3136.875	-167.375	2033	-1616.375	6396.375	501.5	12474.25	1452.5	8718.25	38542.25	4748.5	33133	-997.5	-209.25	799.625	6243.75	2106.125	2143	6827.625	10758.375	41.5	5789.625	764.125	575.125	341	1183.625	1496	1091.125	3005.875	2911.125	488.125	6217.125	37336	70.25	4227.25	195.125	2593.875	890.625	4944.75	3458.625	17232.375	696.375	5558.625	681	4.5	278.5	14845	3406.25	6151.375
SYNZIP5	85.25	7669.375	9659.625	2677.5	-176.25	35912.5	118	4261.25	1387.75	712.75	12771.625	22853.375	2599.375	2408.875	-638.5	33866.875	5001.625	19688.125	-356.25	953.25	33212.875	21966.125	3954.5	1907.375	2968.625	738.875	19386.25	7975.75	6678.5	7283.125	35487.25	30555.25	5312.75	3299.5	1725.625	1474.875	1406.25	740.375	4688.125	30876.75	667.375	616	9197.375	7318.125	370.375	960	333.375	8558.75	6890.5	3569.25	6154.25	7063.125	146.125	11543.625	147	-121.625	-26.625	40014.375	5716.625	4467.875
SYNZIP6	-898.5	8038.125	1564	40661.375	37774	-90.5	-143.125	720.125	3008.5	4376.5	1258.25	2618	4032.5	8001	4907.5	1410.125	19399.5	-173.125	44070.75	33644.25	526.5	-1250	41241.5	16534.5	68.375	165.625	5514.25	8949.25	13667.125	14659.5	15801.375	623.875	7950.125	2593.375	6735.625	2904.625	1100	1450.625	-392	1167.875	-194.875	506.25	17352.125	5085.75	2047.125	-227	144.875	1530.625	44.75	5079.75	4243.625	12134.75	2673.75	16589	-258.625	50451.125	-107.125	-112.625	3719.75	4670.75
SYNZIP7	3491.75	6240.25	-319.25	285.375	-309.125	-559.75	281.75	2372.375	-118.75	135.375	-227.5	-838.5	179	-841	-2143.125	-879.5	115	-773.375	377.125	5980.625	9034.125	3329.875	2323.5	-861	-217.125	552.875	5001.375	3690.25	2588.625	5274.625	41.875	-370.25	2247.25	424.5	91.75	89.125	1726.75	1522.625	1153.375	11141.5	302.875	368.75	5864.375	-716.625	311.625	1454.375	255.875	3570.75	-529	2602.25	32347.25	360.5	4649.375	6636.875	27047.375	-185.5	201.125	-246.75	30001.625	3755.375
SYNZIP8	-26.25	7685.25	1528.5	1877.25	452.25	-27	3148.875	1916	3176.25	5871.5	-138.375	-43.625	-283.125	-37.125	-307.625	2545.875	2857.375	233.375	4890.375	3113.5	8510	3386.625	32177.875	8915.75	-123.375	407.875	7415.25	9124.125	5094	6270.125	1217.75	-82	3136.125	809.5	421.875	116.875	915.5	2925.75	3316.25	10745.125	1110.5	536.375	-190	-44.75	1177.25	2348.875	567	2013.875	819.625	2767	1243.125	2317.875	2708.625	6235.25	1894.25	1311.25	-7.375	125.25	1264.125	2566.5
SYNZIP9	-178.75	3007.25	1339.75	-612.875	854.625	1983.5	58.5	4728.875	653.875	4627	1250.875	2207.625	-836	1389.625	1595.25	5740.875	1029.75	5380.875	2561.5	6657.875	4588.625	-214.625	29461.25	644.375	207.75	558.125	6560.5	7202.875	2679	224.25	2950.75	200.875	1236.5	-117.5	327.125	285.75	24072.75	442.25	1522.25	2002.375	7895.5	688.375	-627.625	1500.625	531.625	2978.125	-632.375	169.875	214.5	34170.875	1541.75	6073.75	24587.625	5738.875	3399.125	1439	19199	2013	1329.5	31369.375
SYNZIP10	310.25	5178.375	211.625	12234	1521.5	4070	1541.625	17712.125	7305.125	-601	2878.25	3540	22523.75	4706.625	-1154.375	16454.375	4745.5	1651.75	-286.375	17169.25	28564.25	22701.625	2167	465.375	455	686	4247.375	239.125	10781.875	7398.875	12440.5	664.75	14952.5	4863.125	7532.375	810.125	1806	1580.25	9100.625	2918.75	1378.125	738	4152.5	1352.25	598.25	2150.875	1645.625	5208	1003.875	1562.625	5436.625	4179.5	-150.5	12891	470.875	2624.5	702.875	4658.375	5082.5	2021.75
SYNZIP11	6169.75	4973.75	5287	10656.25	7699	497.375	1255.125	1310.25	5522.75	766.25	2033.875	122.75	3307.625	8680.25	4114.5	2228.875	10994	934.25	23409.5	30053	32459.125	3536	34355.875	12299.75	584.25	2561.125	22745.5	36794.625	23519.75	21946.875	8404.625	-173.125	31036.25	9121.25	1905.375	620.5	4844.125	12993.5	10133.625	3213	4424.5	1424.5	2567.75	813.25	3601.875	2973.25	1379.125	8323	2010.875	15830.375	17929.375	26643.75	10092	16369.5	4545.5	11578.125	2212	533.5	15494.5	18153.5
SYNZIP12	359	5306	4520.75	9755.375	13703.5	288.375	295.25	911.625	4612	2802.875	99.125	-367.25	21923	21412.875	6919.625	3774.25	15590.75	1723	24047.875	22937.875	16377.625	3419.5	33987.875	15220.625	-41.25	862.125	14693.25	13717.125	12273.5	13080.375	22124.5	2328.125	36988.625	6454.5	4732.875	958.375	1956.875	4639.875	961.5	5161.25	1610.875	1178.625	8583.125	-1728.125	3103	799.75	914.5	5387.5	3180.25	9262.25	12482.625	40057.75	4713.625	11054.25	828.25	17760.875	447.875	850.5	10379.125	10370.5
SYNZIP13	-345.875	32090	10973.75	-2270	360.875	1113	-74.5	167.875	-653.5	12047.625	270.75	14448.375	-785	1039	35569.25	12968.125	-1576.875	10401.125	-1291.125	-849	24996.875	9577.125	9489.625	-210.5	-160.75	558.75	-1246.125	-706.75	3881.125	2904.625	2772.25	81.5	2221.125	16.75	-181.375	-50.125	166.625	-13.875	-2	4561	1019.375	452.125	-1177.125	-100.25	-145	480.375	59.5	351.125	73.625	7393.25	1628.25	11177	-271.5	1128.625	576.625	659.25	-230.875	1800	1851	6599.375
SYNZIP14	308.125	37913.25	7528.25	5078	686.875	3957	194.5	1646.5	1597.25	-41.875	4518.125	21521.875	2938.5	3194.625	20648.25	16603.75	22442.5	10510.875	2516.75	3112	26253.5	21724	36041.875	-114	204.25	970.625	11060.125	6766	8380.375	11584.375	18649.25	916.25	24270	22491.25	2464.875	2040.5	5534.25	3229.25	1917.875	11333.5	2611.125	759.25	3923.625	3037.875	668.75	1356.375	442.125	19711	1634.625	6924.75	9191	9794.875	2727	8261.75	303.5	1466	2471.625	5248	5608	7193.125
SYNZIP15	608.5	409.875	2844.25	-1704.5	-328.375	516	-207.75	-233	-1521	-1778.5	1994.25	4332.375	36848.625	13204.5	-1832.25	11318.75	14731.875	537.625	1312	834.75	35396	7230.5	17382.25	5704	217.5	963.25	26415.875	19114.125	9017.75	8936.125	48837.375	13359.5	43436.25	36460.25	638.5	336.75	3790	1328.875	-287.375	1684.625	-313.125	224.625	17729.875	-1455.625	-297.375	1080.5	649.75	15768.75	5377.75	8950.375	35747.25	14239.875	-629.875	1597.125	342.875	-426.375	1037.75	393.625	26273.625	8321.75
SYNZIP16	1200.75	14994.5	5220.25	4013.25	17575.625	199.625	538.125	1751.375	3404.125	2502.75	564	1005.375	8469.75	7710	5484.375	9851.5	12009.5	2442.25	15363.25	30927.25	27027.5	7271.75	42243.625	21729.125	-83.75	602.875	15216.625	20446.125	9539	10450.5	7936.625	484	34066	7310.625	1855.375	407.25	9738	3304	4137	14315.5	22046.625	942.625	1694.25	1519.625	5918.5	1485	1025.625	5514.125	1104.875	11950.5	20306.625	10669.375	10058.125	16018.125	4126	23360.75	5900.25	253.25	16289.125	14487.625
SYNZIP17	26.75	9431.25	14422.125	1381.75	759.125	5368.625	300.875	4604	136.125	1475.5	4598	9530.75	382.25	12973	31507.625	16546.875	2430.875	29468.875	51.5	4942.625	35158.75	1022.375	22352	3058.125	403.5	750.875	5285.75	7445.25	2337.75	1693.5	9065.25	360.875	7464.875	724.25	655.75	1238	33626.5	624.375	4377.625	1317.375	13695.875	551.625	0.5	10334.5	1269.25	7741.75	198.125	-279.5	1423.375	31131.5	951.125	3487.125	20467.5	4762.5	351.75	1223.625	23343.125	5787.125	1121.75	31600.125
SYNZIP18	-424.375	2586.25	-4.25	23264.625	12069	-291.625	-150.5	1529.375	9335.625	-397.75	2356.875	2288.875	17480.25	10362.875	2825.375	10579	34443.25	195	34738.625	19722.25	9645.75	1627.75	33912.25	10686.875	-1031.125	533.125	14059.375	9643.875	12798	16171.625	16593.375	401.875	10363.25	9376.25	19906.75	3726.375	5216.5	3350.5	551.875	12116	-254	671.25	18844.875	883.375	2713.875	309.375	1966.625	6394.5	-55.25	2034	8274.375	5824.833	4007.5	19155.375	956.125	17117.375	2225.75	109.875	5166.625	1663.5
SYNZIP19	5755.75	45176.875	2068.125	2440.875	-115.875	20840	680.125	11074.75	2522.125	-532.125	15415.875	25068	955	470	-974.5	38380.875	2777.25	45298.125	-969	-607.125	49971.5	31356.625	1179.25	-182.375	2028.25	958.25	2979.125	34.875	5165.875	6621.75	16170	1115.5	43399.25	11110.5	2646	1352.25	7652.125	2448.25	6755.625	32438.875	3142.375	542.125	533.75	6987.875	457.375	2429.125	106	9506.125	20530.625	11655.875	4515	7485.125	259.375	265	388	-200.125	3888.125	19731.625	4373.375	11508.875
SYNZIP20	2040.5	49162.375	6805.75	3834.125	-348.5	19414.875	3515	2430.625	2857.625	6797.75	41208.5	43431.375	628.25	641.125	1738.25	39021.5	5128.875	43702.375	-806.25	5974.625	36110.625	15364.5	18270.125	1188.875	8618.625	1781.625	15086	-648.75	1156.75	2391.25	15291.25	2172.875	9773.375	4216.125	4062.125	7885.25	-383.25	307	456.375	9689.25	2605.5	439.875	-142.375	3469.25	271.375	1832.625	1090.25	5166.875	5052	17962.25	4251.125	15726.5	-88.875	3124.25	1787.875	-52	-718.125	20718.625	3381.25	19099
SYNZIP21	-563	6872.25	2657.125	30320.75	25120.125	-154.875	4659.875	4335.875	1424.125	13937.75	19684.5	9979.75	20943.25	15840	27662	24776.875	22328.25	3974.25	36175.25	22019.375	5635	3822.375	38270	21588.25	572.75	632.125	220.25	766.875	2907.25	2997.25	19554.875	6103.375	13281.25	8181.75	9571.625	5215.875	1600	1910	170.75	698.25	351	566.75	2579.75	699.25	900.5	1037.25	7398.25	3473.25	2297.25	4793.875	3314.125	32347.375	1111	27319.5	1097.125	31805.625	-131.25	651.125	3480.75	4989.25
SYNZIP22	20784	19647.125	3614.25	2006.125	17091.25	392.375	6791.75	11137.5	1996	27744.875	4447.5	6560.75	13293.5	44903.875	22642	17881.125	8033.25	5696.25	39174.625	29506.875	16302.625	1366	33168.25	22768.5	631.625	961.125	7654.75	18178.25	8721.25	11848.625	15375.875	1028.125	31330	5762.5	7432.125	511.75	6781	5398.75	2886.875	5431.75	14364.25	7311.875	6067.875	1502.625	10906.75	6275.875	979	2258.125	6420.5	18413.125	46531.625	16363.625	15474.125	26119.5	28539.25	20949	2210.375	-128.5	37329.75	19989.5
SYNZIP23	4067.875	20087.75	2195.25	13143.875	491.75	24128.625	2195	50967.75	16428.875	242.625	16873.25	34517.625	4931.125	23576.75	26741	48678	12428.25	37390.125	-662.5	14160.875	46508.25	18793.375	-635.25	9376.5	1206.625	2496.375	126.5	-1312.75	3667.125	2347.25	47534.875	4024	20924.125	22911.25	11860.375	25743.875	357.25	854	2202.75	11532.5	262.375	459	20967.5	25367.25	722.125	5010.5	1245.375	4291	41325.625	25403.375	3541.75	19932.625	7074.375	2978	2526.375	688.625	-243.125	24579.375	3239.375	25406.375
SYN24	-757.125	46231.875	-287	-2798	-794.25	649.125	-352.375	3943.875	-546.375	-624.5	1719.25	8750.375	-639.75	-1220.75	325.375	21574.25	-1315	2602.5	-1666.125	-2221.75	42194.25	8413.75	420.75	10344.25	70.125	-32.125	3985.25	-221.5	-11.875	-343.625	25124.875	6517.875	1311.625	3093.5	-520.25	-458.875	1583.375	1664	533.375	17240.625	-121.375	301.25	-906.75	-1086.875	-153.375	1198.875	-424	478.125	1389.375	-557.125	1939.875	365.5	-1420.375	-284.625	171.875	-707	308.25	771.25	2117.375	-651.625
SYN25	1703	-228.875	-495.75	4192.5	4468.375	-290.25	-310.75	-304.875	244.75	-391.375	-351.75	-629.125	1032.625	510.875	-2561.625	-1163.625	1746.75	-606.75	12561.625	20570.875	1140.25	-993.625	7693.125	2440.75	-70.5	377.125	4227.5	7108.25	15053.75	13857	1985.25	-32.375	26088.75	-31.375	-6	9	347.875	945.5	438	492.875	193.625	621.75	-339.625	-1308.75	992.125	-852.375	673	4632.375	125.375	14939	3907.125	7493.25	357.75	3463	246.875	7360.125	-180.375	-351	3354	14167.5
SYN26	243.25	157	-176.75	348.125	-292.75	2291.875	32.625	734.25	-365.375	-740.625	1319.75	150.625	1725.375	-95.625	-402.125	1.375	-368.625	12.625	1905.375	3065.75	3487.375	-1153.125	9555.625	-571.5	3731.25	1079.375	-2087.25	-1663.625	700.375	895.25	918.75	-265.875	590.875	214.875	333.25	890.375	100.125	88.125	-298.25	-239.625	-115.75	323.625	-114.75	359.5	-178.75	-19	531.75	9262	721.875	1261.875	1364.125	743.75	1003	1360.75	300.125	848.75	-158.75	58.5	1260.375	407.625
SYN27	389.125	5852	855.125	5952.375	2178.75	1826.25	1518.25	3726.25	988.25	313	5058	2295.75	501.75	5619.5	15248.875	9462.125	3089.625	1459.375	629	6337.5	1197.625	-120	1155.75	5261	373	946.25	15214.5	11332.875	2437.875	1684.125	5682.875	676.125	2856.25	1714.875	922.75	888.25	21756.125	1749.375	4126.5	6724.75	24764.75	982.25	271.375	2822.125	3689.875	5945.75	258.375	224.25	1233.375	11190.875	3004.25	3749.125	20822.875	1764.25	1659.875	3435.125	15729.625	2018	2248.625	12173
SYN28	-451.625	6751.75	14.125	2456.375	331	2174.5	822.125	2946	482.75	-569.5	4881.375	945.25	-94.875	2150.75	8602.875	11086.875	1900.75	744	-1211.125	-564.625	715.125	-157.5	-1390.5	1587.625	245.625	530.25	10344.375	4448.125	931	521.25	1914.5	61.75	2431	530.25	-86.625	522.875	12196.5	631.25	4580.25	6693.375	6882.5	577.875	-385.625	1292.75	947.5	6163	-24.625	-361.5	796.625	7196.625	1807.125	2316.75	10386.25	-42	1139	716.5	6897.75	2023.375	1833.125	8138.25
SYN29	1896.875	30870.25	1920.75	1975	3266.125	9225.5	3999	12211	1676	7345.75	20577.625	14436.875	3188.5	10125.25	14839	25111.375	3769.75	16366.75	581.5	6595	10481	9108.25	12240.75	5028.875	14431.5	424	8083.5	6141.875	416.375	640.5	6525.875	4252.625	12063.375	3571.125	103.375	758.75	15566.375	4197.25	4578.875	9246.5	13843	4461	1072.875	10681	4194.5	12912.875	99	-131.375	5111.25	9189.125	8674.375	4866.25	11467.625	9058.375	5495.75	4790.625	14756.75	9066.625	6620	11400.375
SYN30	4521.875	24828	2650	13367	3763.5	15017.75	8682	19723.5	661.875	9620.875	21824.875	15677.25	5439.25	15343.75	29943.25	23308.125	3590.75	23744.375	6878.875	6579.25	14194.375	10006.625	16090.375	10835.125	12132.375	778.25	1441.375	229.875	426.5	1630	11833.875	3705.125	12311.5	6951.125	7601.25	7576.125	5188.375	2818.125	5833.5	6277.875	12834.625	1001.375	5983.5	16354.25	5876.75	23510.625	808.125	859.125	7876.75	12206.125	12458.875	7376.375	17800.75	11935.875	9128.625	6310.125	2989.5	15460.125	10116.75	13449.375
SYN31	-227.625	4698.125	192.875	-476.5	3162.625	92.5	-91.375	-141.625	-156.5	490.875	248.25	3610.625	-657.25	2890.5	17842.75	2402.25	-785	1358.625	803.875	5209	9598.75	435.625	23329.625	16403.5	-92	177.125	419.5	669.75	798	375.875	12845.75	820.75	5088.25	22225.5	96	848	1488	474.875	-209.125	247.125	-221.875	296	1153.375	1996.75	230.125	9	102.75	-633.5	2210.5	-26	6120.75	2839.375	206.75	3165.5	13.125	3248.25	223	44.75	4529	364.625
SYN32	-1281.125	1743.375	-1031.375	-4299.875	6521.25	9.375	-152.75	-259	-593	-526.375	-227.75	279.5	-1209.75	323.375	11618.25	162.5	-1720.125	-391.875	1243.25	1323.25	7954.625	-1280	4434.875	9960.375	-93.5	964.375	4821.875	3274.625	2862.25	1435.375	5780.625	303.625	1929.5	21185.625	-404.625	249.875	764.875	1464.5	2267.75	-236.5	-987.5	395	-1065.25	-552.375	228.25	319.125	116.125	-60.875	1737.25	4674.125	5014.25	7568	66.875	6813.875	632.125	9805.375	63.875	-606.75	4410.875	12184
SYN33	-354.875	25369.25	1083.875	334.625	316.5	845.625	1766.375	2265.875	317	4585	12673	22749.5	307.25	22381.75	27053.125	24659.375	5735.125	4350.375	13702.875	7584	14104.125	9135.125	14963.875	5618.375	7911	331.875	5119.875	10270.75	3513.125	1894.125	13516.75	2042.75	18294.625	21285.5	947.5	2015.875	2558.375	1247.875	3484.625	4232.375	3187.5	954.25	2582.5	860.75	5600.125	959.5	147.5	3504.75	1597.625	4427.875	18008.375	4339.375	4169.5	8353.5	8524.75	824.875	817.75	978	13227	4968.375
SYN34	119.5	4531.625	3470.75	1309.25	514.25	513.375	3.125	350.125	-146.375	612.875	3235.875	2524.25	748.375	20234.375	40815	8797	927.875	3038.125	2890.875	4347.75	10535.125	2697.25	28266.875	8234.625	227.5	743	2034.125	658.375	2390.75	3495.5	41747.5	36836	39042.875	10390.375	274.5	734.25	3025	1614.25	925.375	1853.875	1148.75	491.875	547.75	535.125	378.25	1169.25	228.625	693.125	13095.25	8182.75	17674.75	19232.875	675	5185.25	1235.25	717.375	1362	505	14255.25	9653.875
SYN35	427.625	1246.75	16456.75	1286.875	655.375	3118.75	255.375	588	87.375	2182.125	976.75	-495.75	374.25	1183.75	1481.375	3338.875	2659.625	10191.5	3651.375	7530.125	17653.875	1099.125	26860.625	923	151.25	874.5	2715.375	-240.625	2466.875	7036.125	4433.375	-63.125	2486.875	677.125	1358.75	677	1555.625	1583.25	1357.125	3599.25	5301.625	545.25	708.5	3017.875	142.125	465.875	299.5	1453.125	295.875	3024.125	1989.5	2626.625	5027.75	2326.625	1194.5	935.625	728.25	3840.125	1924.25	3736.625
SYN36	-71.875	-324.25	311.875	-1904.875	-132.75	772.25	-62.125	92	-371	-196.75	-139.625	128.375	-523.375	-231.75	-996.875	-405	16.375	490.75	506	2182.875	1569.75	-1066	11293.375	-1201.375	34.75	388.125	791.25	173.5	1053.375	2300.5	2821.875	171.75	1090	587.625	174.5	843.125	572	471.25	65.625	-103.375	418.375	461.375	662.125	1624.375	75.5	-98.625	52.75	959.25	-0.875	638.75	1753.625	3381.125	1060.75	1372.875	507.875	-205.5	-58.25	1580.75	1919.25	863.5
SYN37	-141.625	8759.5	-522	220.875	-456.25	-663.625	544.5	148.5	8519.125	-415.375	44.25	-426.375	14.125	39.5	627.375	8424.375	15728.625	366.5	3770.25	-1960.5	987.375	-1737.875	-893.75	1978.5	61.375	596.75	32892.125	18435	4601.333	1977.875	1434	39.25	596.25	1546.25	406.375	75	2358.875	2354.375	4380.625	4384.5	849.125	551	-685.5	-691.375	601.5	1419.5	483.125	-43.25	-23.875	4497.625	1973.375	1903.75	4773.25	2179.625	1959.75	-202.5	439.5	176.375	2504.375	4514.625
SYN38	57	404.875	1296.625	2669	37.5	103.875	983.75	1996.625	-247.875	-24.625	3164.25	-37.125	181.875	7925.25	2440.625	4952.875	879.75	-34.875	1560	-555.25	2810.875	-388.875	2498.375	11068.375	171.5	967.25	6707	6157.875	2708.75	2190.375	4101.5	-46.25	4548.375	3334.125	746.875	452.875	9506.25	3193.125	2086.75	3038.375	23897.875	650.625	-91.5	-75.625	2717.25	692.5	-26.75	484.75	9668.5	18673.125	2727	4894.375	4388.75	1231.75	772.25	275.125	3456.75	-287	2642.375	19993.125
SYN39	-191	3869.125	847.875	2954.25	365.875	-3.75	1788.625	3831.75	916.25	1073.125	3212	266.125	-453.125	1242.125	762.125	6160	3434.375	19.125	4787.5	1473.875	1328	-109	5792.25	3799.375	-305.5	572.75	9844.25	12439.875	3262.125	4044.125	1774.625	219.625	2998.25	1040.875	1274.75	333	8809.625	2277.125	9723.125	3486	2346.75	596.25	25.5	-97	951.75	5209.25	325.875	762	227.5	10208.5	2422	3492.333	7314.25	4994.75	77.75	907.625	4679.5	366.75	958	12813.875
SYN40	137.375	2158	-158	2992.25	10116.625	237.25	8195.375	8907	-131.875	-811.625	692.875	236.75	648.75	7773	1464	18851.25	301.75	2569.125	13835	7316.375	-276.5	-659.125	8391.625	26446.125	138.375	849.125	10091.625	17681.625	2758.875	1056	1426	-143.125	3572.25	243.25	2184.625	173.75	7521.75	2104.375	1557.375	14896.5	3498.375	6775.5	-4647.75	-1083.75	831.5	2152	430.75	38.25	-121.375	3875.375	13239	-896	7118.125	2705.5	1785.125	12696.75	2756.125	-333.625	10121.5	6037.25
SYN41	-1118.5	1083.125	-182.875	2248.125	-303.75	-229	415.625	544.5	2035.375	-991.5	54	128.25	-254.625	-831.75	-1632.625	15347.375	6736.625	-357	1778.875	960.375	-130.5	2339.125	-1279.125	555	68	315.375	30882.25	13176.75	4472.75	2349.375	794.125	-38.5	2688.25	321.5	2607.5	169.375	1699.875	1982.125	1782.625	3529	13639.875	1222.625	-454.875	-401.875	787.5	-185.875	-12.75	-303.75	-158.75	1074.625	669	536.75	948.75	424.5	459.625	-156.75	-288.125	-115.5	1025.125	1602.375
SYN42	35.875	788.375	408.625	-90.375	-124.75	102.75	26.875	300.375	34.125	-209.5	150.625	-51.125	161.75	-673.875	-871.5	1826.125	831.5	-423.5	-838.625	-548.25	-69.375	6331.875	-171.375	652.375	192.25	986.375	4210.125	237.375	5146.625	2024.375	1770	-530.875	1984.75	322.25	290.25	316.625	1136	540.125	592	19532.25	4762.625	695.25	0.5	-99.25	80.375	-108	140	85.875	-292.125	2172.25	4351.125	746.25	338.25	358	813.25	95.125	455	17.375	3206.25	2475.875
SYN43	-934	15741.5	10102.125	4654.25	2996.875	4873.75	4742.375	68	-238.5	1651.875	132.75	3818.125	-337.125	2192.5	26601.875	2690.25	-751.5	6669.625	-707.125	511.5	11665.75	2572.125	34636.5	12303.625	112.875	339	-1211.5	-1321	1187.5	2325.75	9910.25	179.625	4927.75	366.625	416.125	701.125	984.875	246.875	-91.375	1951.25	822.125	420.75	-811.25	30243.875	352.25	6761.5	63.25	-58.25	706.625	3319.25	2988.875	9388.375	-141.5	1247.625	221	3747.75	145	5225.25	2600.875	3998.125
SYN44	-190	441.75	-258.375	38735.125	3533.25	1397.5	-129.625	-180.25	3271.5	306.5	813.25	-423.125	1070.5	4856.375	-544.75	2946.25	11164	38.125	9649.875	7054.625	1918	23.625	28527.5	2598.5	548.75	574.625	11327.625	10547.125	7743.5	8754.5	16103.5	1072	5818.875	2281.125	7600	4859.625	716	1479.25	96.125	2382	-230.125	335.625	33033.25	9029.125	512.125	1088.625	2209.625	1393.5	202	1035.5	5835.25	8621.625	403.625	5087.125	71.375	5305.875	-94.75	798	5829.625	1247.5
SYN45	-175.625	4051.875	672.5	707.75	-535	1052.375	67.75	1818.75	430.375	-403.25	1308.75	1357	-60.5	-119.125	-2049	10866.875	1885.75	742.625	464.625	-100.375	1837.75	3990.25	1966.25	-392.25	-268.25	754.75	12878	5165.75	2977.625	5765.875	4293.375	149.875	7143.375	1168	87.375	290.25	1092.25	3241.375	2472.375	3650.75	490.5	526.25	1257	-192.375	709.75	328.25	70.5	819.375	68.25	3057.625	3345.875	7287.25	1439.125	4763	199.625	77.625	239	1796.25	1648.875	4256.125
SYN46	2115.75	-620	-932.75	-914.25	-506.375	-383.375	-100.375	-75.875	-126	-163.25	-700.5	-987.5	-701.125	-1094.125	-5031	-1059.5	-806	-777.125	-261.875	-160.625	-1490.75	-2292.125	-1062.375	-545.75	-196.125	63.375	2680.25	3731.375	1810.25	1776.75	-1576	-56.125	-1184.875	-1889.375	-99.75	-168.125	249	230.625	193	-247.75	-522.25	227.5	436.625	-2569.125	338.375	1545.875	10.5	5615.125	-214.125	-678.75	-419.75	-462.625	355.125	1211.5	833.625	-538	-79.25	-553.25	400.125	-244.375
SYN47	27.875	-97.625	306.125	-1210.625	-298.75	1398.625	-277.5	590.875	-366.625	-503.75	765.25	20.125	487.125	-302	-592	-337.25	-1327.625	-42.75	-591.375	1623.75	9564.625	-1087.5	871.25	-1214.125	4208.75	255.125	-2068.125	-636.125	338	352.625	576.25	51.75	-43.125	-216.5	-200	64.25	356.875	369	-1236.5	-264.625	-222.625	273.625	-104.25	398.875	-310.75	-296.75	128	8248	332.375	746.875	686.75	660	4774.5	453.25	-300	211.75	-673	122	521.875	77.375
SYN48	5590.125	10726.875	904.125	1250.625	2799.625	1541.625	4291	7820.875	-245.5	5330.5	7251.125	5793	184	6076.375	10075.75	4610.25	-1247.5	6124.125	3850.25	3134.5	5566.875	686.125	2989.5	483.375	3965.875	12198.75	-2002.125	-1452.5	-217.125	-60	2622.125	178	6620.375	639.5	1486.125	3665	768.375	806	709.625	1509.875	-348.5	458.625	-195.25	2779.75	1187.375	12065.75	21439.125	2571.625	1855.375	2462.5	5761.375	2081	10982.625	1879.25	1272.75	4041.875	115.375	1665.5	4930.125	2420
BATF	169	4108	289.5	3800.625	1982.625	122.5	483.375	640.125	273.375	188.625	1846.875	673.875	539.25	883	5957.125	2534	3008.625	-212.5	16793.125	7000.75	3581.375	3339.625	38364	5683.25	187.625	757.25	7114.875	8121.625	5987	6497.375	13330.5	1540.5	3127.125	17304.875	584.5	582.625	1721.875	10870.375	1694.375	1011.375	715.125	480.75	1645.875	-484.75	421.5	664.25	346.75	949	671.875	1091	8019.125	7824.875	4464.75	35898.75	1824.625	2706.25	768.125	-666.75	7322.875	2072.75
FOS	355.875	25811.125	438.125	4373	353	823.375	1809.375	1107.125	31699.625	-516.125	6157.875	1934	2685	6466.375	5057.375	28581.75	37108.25	117.75	6972.75	25938.125	7486.625	12546.75	26601.625	534	1413.375	1068.875	24859.875	19649.75	8339.75	5178.5	1853.375	816.375	5876.875	10360.375	2255.375	724.875	7880.875	13262.125	12213.875	5632.25	1418.5	973.25	-145.625	-163.25	614.875	3601.5	661.75	383.25	183	2417.625	6565.625	3277.875	2061.5	26790.75	676.125	660.625	2984.5	876.5	5317.75	3855.875
ATF4	341.25	45201.25	3634.5	1430.25	703.5	443	36041.125	476.25	-387.25	481.125	10480.875	6243.875	520.25	8382.375	49513.375	41931.125	346.125	1062.125	294.125	838.875	4479.125	30585.875	7694.125	11346.5	288	777.375	3533.25	1365.625	8279.625	6124.75	32811	1242.875	27808.25	28253	260.375	569.75	1829.75	349.125	528.375	21756.25	125.125	926	941.5	3857.75	412.125	2929	258.25	2005.5	5058	5382	881.5	15257.625	2381.25	1593	8034.375	1142.5	1138.25	119.25	683.875	6049.25
ATF3	-158.75	17343.625	891.5	8663.75	369.25	1460.875	363.5	598	670.875	220.25	6402.125	19974.75	4257.375	4087.5	4948.375	12070.25	2376.5	214	1093.375	13519.375	29434.75	7975.75	24547	1577	106	1185.75	2495	1887.5	3678.875	4279.75	9108.125	1161.75	3026.875	14628.5	1130.875	994	2252.875	2349.75	3975	1357.75	908.25	512.875	2961.375	1974.875	1449.75	370.625	678.5	-242.5	1625.75	3603	9937	1793.75	491.5	20496.375	-409.25	1160.75	1131.5	1854.125	6762.875	3957.625
BACH1	452.375	2642.625	-1.375	4098.125	39	366.75	2991	1942.25	8760.5	-308.875	1788.75	-636.5	615.5	2117.125	-2430.75	7640.75	10141.125	-480	543.75	-1276.625	919.375	3805.875	6787.625	-99	1584.75	1866.25	30298.125	22918.75	4367.125	4725.75	2206.75	-234.625	1996.25	1235.125	3108.25	801.125	10083.25	2518.875	6443.375	6296.5	1611	930	-0.375	-1432.5	1162.5	3202.625	11239.75	1899.875	966.375	2435.125	3553.5	472.5	3295.625	7532.25	524	170.125	5262.875	283	3410	4463.375
JUND	271.25	2510	12860.5	2623.375	832.25	3651.625	795.625	3186	878.125	1003.75	506.875	-1547.75	1265.375	-289.25	-458.25	14361.875	2505.5	1165.75	-1055.625	2079	29895.625	10619	7296.25	697.5	20.375	1306.875	-1786.125	-1311	4660	4605.25	18241.625	300	8043.875	2521.25	224.5	403.5	-13.25	292.25	418.375	1418.75	-31.375	601.25	-140.125	-861.375	225.75	345	303.125	1184.25	17584.125	22293.125	987.375	25712.75	-84.5	2800.75	25.625	1688.75	87.5	2166.75	1413.125	22039.5
NFE2L3	134.25	-858.25	-336.5	-580.875	-133.25	83.75	4285.5	165	327.625	-171.625	30.75	-417.5	98.125	-792.125	-804.375	-560.625	-524	-538.875	-1534.5	-1125.375	-1093.875	3456.125	-1738.75	-185.5	186.75	-105.875	-491.25	-1419.5	269.5	603.25	624.75	-494.75	821.625	-249.625	229.875	349.5	126.875	-152.25	-109.25	326.75	-994.75	291.25	-21.875	-611.5	0.75	265.875	55.75	-742.75	-260.25	-1926.125	1456.375	-1875.375	-295.25	-1931.25	382.125	-293.5	272.5	-146.75	1664.375	-1536.875

A synthetic coiled-coil interactome provides heterospecific modules for molecular engineering

A.W. Reinke, R.A. Grant & A.E. Keating

Table S3. List of the proteins composing each of the subnetworks identified.

2-nodes	Motif	A	B		
pairs	A-B	SYNZIP5	SYNZIP6		
pairs	A-B	SYNZIP20	SYNZIP11		
pairs	A-B	SYNZIP20	SYNZIP16		
pairs	A-B	SYNZIP20	SYNZIP2		
pairs	A-B	SYNZIP13	SYNZIP15		
pairs	A-B	SYNZIP16	SYNZIP23		
pairs	A-B	SYNZIP12	SYNZIP23		
pairs	A-B	SYNZIP22	SYNZIP19		
pairs	A-B	SYNZIP22	SYNZIP14		
pairs	A-B	SYNZIP22	SYNZIP10		
pairs	A-B	SYNZIP22	ATF4		
pairs	A-B	SYNZIP2	SYNZIP14		
pairs	A-B	SYNZIP2	SYNZIP1		
pairs	A-B	SYNZIP19	SYNZIP18		
pairs	A-B	SYNZIP19	SYNZIP21		
pairs	A-B	SYNZIP15	ATF4		
pairs	A-B	SYNZIP9	FOS		
pairs	A-B	SYNZIP17	SYNZIP18		
pairs	A-B	SYNZIP17	FOS		
pairs	A-B	SYNZIP18	SYNZIP23		
pairs	A-B	SYNZIP23	SYNZIP21		
pairs	A-B	SYNZIP23	SYNZIP6		
pairs	A-B	SYNZIP23	SYNZIP8		
pairs	A-B	SYNZIP23	BATF		
pairs	A-B	SYNZIP21	SYNZIP4		
pairs	A-B	SYNZIP3	SYNZIP4		
pairs	A-B	SYNZIP7	ATF4		
3 nodes	**Motif**	**A**	**B**	**C**	
line	A-B-C	SYNZIP5	SYNZIP6	SYNZIP5	
line	A-B-C	SYNZIP11	SYNZIP20	SYNZIP16	
line	A-B-C	SYNZIP11	SYNZIP20	SYNZIP2	
line	A-B-C	SYNZIP20	SYNZIP2	SYNZIP14	
line	A-B-C	SYNZIP20	SYNZIP2	SYNZIP1	
line	A-B-C	SYNZIP13	SYNZIP15	ATF4	
line	A-B-C	SYNZIP16	SYNZIP23	SYNZIP16	
line	A-B-C	SYNZIP16	SYNZIP23	SYNZIP16	
line	A-B-C	SYNZIP16	SYNZIP23	SYNZIP6	
line	A-B-C	SYNZIP16	SYNZIP23	SYNZIP8	
line	A-B-C	SYNZIP16	SYNZIP23	BATF	
line	A-B-C	SYNZIP12	SYNZIP23	SYNZIP12	
line	A-B-C	SYNZIP12	SYNZIP23	SYNZIP6	
line	A-B-C	SYNZIP12	SYNZIP23	SYNZIP8	
line	A-B-C	SYNZIP12	SYNZIP23	BATF	
line	A-B-C	SYNZIP19	SYNZIP22	SYNZIP14	
line	A-B-C	SYNZIP19	SYNZIP22	SYNZIP10	
line	A-B-C	SYNZIP19	SYNZIP22	ATF4	
line	A-B-C	SYNZIP14	SYNZIP22	SYNZIP10	
line	A-B-C	SYNZIP10	SYNZIP22	ATF4	
line	A-B-C	SYNZIP14	SYNZIP2	SYNZIP1	
line	A-B-C	SYNZIP19	SYNZIP18	SYNZIP19	
line	A-B-C	SYNZIP19	SYNZIP18	SYNZIP23	
line	A-B-C	SYNZIP18	SYNZIP19	SYNZIP21	
line	A-B-C	SYNZIP19	SYNZIP21	SYNZIP19	
line	A-B-C	SYNZIP19	SYNZIP21	SYNZIP4	
line	A-B-C	SYNZIP15	ATF4	SYNZIP15	
line	A-B-C	SYNZIP9	FOS	SYNZIP9	
line	A-B-C	SYNZIP18	SYNZIP17	FOS	
line	A-B-C	SYNZIP18	SYNZIP23	SYNZIP21	
line	A-B-C	SYNZIP18	SYNZIP23	SYNZIP6	
line	A-B-C	SYNZIP18	SYNZIP23	SYNZIP8	
line	A-B-C	SYNZIP18	SYNZIP23	BATF	
line	A-B-C	SYNZIP21	SYNZIP23	SYNZIP6	
line	A-B-C	SYNZIP21	SYNZIP23	SYNZIP8	
line	A-B-C	SYNZIP21	SYNZIP23	BATF	
line	A-B-C	SYNZIP6	SYNZIP23	SYNZIP8	
line	A-B-C	SYNZIP6	SYNZIP23	BATF	
line	A-B-C	SYNZIP8	SYNZIP23	BATF	
line	A-B-C	SYNZIP21	SYNZIP4	SYNZIP21	
4 nodes	**Motif**	**A**	**B**	**C**	**D**
2 pairs	A-B,C-D	SYNZIP5	SYNZIP6	SYNZIP13	SYNZIP15
2 pairs	A-B,C-D	SYNZIP5	SYNZIP6	SYNZIP1	SYNZIP2
2 pairs	A-B,C-D	SYNZIP5	SYNZIP6	ATF4	SYNZIP15
2 pairs	A-B,C-D	SYNZIP5	SYNZIP6	FOS	SYNZIP9
2 pairs	A-B,C-D	SYNZIP5	SYNZIP6	SYNZIP7	ATF4
2 pairs	A-B,C-D	SYNZIP20	SYNZIP11	SYNZIP15	SYNZIP13
2 pairs	A-B,C-D	SYNZIP22	SYNZIP19	SYNZIP3	SYNZIP4
2 pairs	A-B,C-D	SYNZIP22	ATF4	SYNZIP3	SYNZIP4
2 pairs	A-B,C-D	SYNZIP2	SYNZIP1	SYNZIP21	SYNZIP4
2 pairs	A-B,C-D	SYNZIP2	SYNZIP1	SYNZIP3	SYNZIP4
2 pairs	A-B,C-D	SYNZIP15	ATF4	SYNZIP3	SYNZIP4
2 pairs	A-B,C-D	SYNZIP9	FOS	SYNZIP21	SYNZIP4

2 pairs	A-B,C-D	SYNZIP9	FOS	SYNZIP3	SYNZIP4	
2 pairs	A-B,C-D	SYNZIP9	FOS	SYNZIP7	ATF4	
2 pairs	A-B,C-D	SYNZIP17	FOS	SYNZIP7	ATF4	
2 pairs	A-B,C-D	SYNZIP23	SYNZIP6	SYNZIP7	ATF4	
2 pairs	A-B,C-D	SYNZIP23	SYNZIP8	SYNZIP7	ATF4	
2 pairs	A-B,C-D	SYNZIP3	SYNZIP4	SYNZIP7	ATF4	
hub	A-B,A-C,A-D	SYNZIP2	SYNZIP1	SYNZIP20	SYNZIP14	
hub	A-B,A-C,A-D	SYNZIP23	SYNZIP16	SYNZIP12	SYNZIP18	
hub	A-B,A-C,A-D	SYNZIP23	SYNZIP6	SYNZIP12	SYNZIP16	
hub	A-B,A-C,A-D	SYNZIP23	SYNZIP8	SYNZIP12	SYNZIP16	
hub	A-B,A-C,A-D	SYNZIP23	BATF	SYNZIP12	SYNZIP16	
hub	A-B,A-C,A-D	SYNZIP23	SYNZIP6	SYNZIP18	SYNZIP16	
hub	A-B,A-C,A-D	SYNZIP23	SYNZIP8	SYNZIP18	SYNZIP16	
hub	A-B,A-C,A-D	SYNZIP23	BATF	SYNZIP18	SYNZIP16	
hub	A-B,A-C,A-D	SYNZIP23	SYNZIP8	SYNZIP16	SYNZIP6	
hub	A-B,A-C,A-D	SYNZIP23	BATF	SYNZIP16	SYNZIP6	
hub	A-B,A-C,A-D	SYNZIP23	BATF	SYNZIP16	SYNZIP8	
hub	A-B,A-C,A-D	SYNZIP23	SYNZIP6	SYNZIP18	SYNZIP12	
hub	A-B,A-C,A-D	SYNZIP23	SYNZIP8	SYNZIP18	SYNZIP12	
hub	A-B,A-C,A-D	SYNZIP23	BATF	SYNZIP18	SYNZIP12	
hub	A-B,A-C,A-D	SYNZIP23	SYNZIP8	SYNZIP12	SYNZIP6	
hub	A-B,A-C,A-D	SYNZIP23	BATF	SYNZIP12	SYNZIP6	
hub	A-B,A-C,A-D	SYNZIP23	BATF	SYNZIP12	SYNZIP8	
hub	A-B,A-C,A-D	SYNZIP22	SYNZIP10	SYNZIP19	SYNZIP14	
hub	A-B,A-C,A-D	SYNZIP22	ATF4	SYNZIP19	SYNZIP10	
hub	A-B,A-C,A-D	SYNZIP23	SYNZIP6	SYNZIP18	SYNZIP21	
hub	A-B,A-C,A-D	SYNZIP23	SYNZIP8	SYNZIP18	SYNZIP21	
hub	A-B,A-C,A-D	SYNZIP23	BATF	SYNZIP18	SYNZIP21	
hub	A-B,A-C,A-D	SYNZIP23	SYNZIP8	SYNZIP18	SYNZIP6	
hub	A-B,A-C,A-D	SYNZIP23	BATF	SYNZIP18	SYNZIP6	
hub	A-B,A-C,A-D	SYNZIP23	BATF	SYNZIP18	SYNZIP8	
hub	A-B,A-C,A-D	SYNZIP23	SYNZIP8	SYNZIP21	SYNZIP6	
hub	A-B,A-C,A-D	SYNZIP23	BATF	SYNZIP21	SYNZIP6	
hub	A-B,A-C,A-D	SYNZIP23	BATF	SYNZIP21	SYNZIP8	
hub	A-B,A-C,A-D	SYNZIP23	BATF	SYNZIP6	SYNZIP8	
line	A-B-C-D	SYNZIP5	SYNZIP6	SYNZIP23	SYNZIP8	
line	A-B-C-D	SYNZIP13	SYNZIP15	ATF4	SYNZIP7	
line	A-B-C-D	SYNZIP19	SYNZIP21	SYNZIP4	SYNZIP3	
box	A-B-C-D-A	SYNZIP21	SYNZIP23	SYNZIP18	SYNZIP19	
5 nodes	**Motif**	**A**	**B**	**C**	**D**	**E**
pair+line	A-B,C-D-E	SYNZIP5	SYNZIP6	SYNZIP13	SYNZIP15	ATF4
pair+line	A-B,C-D-E	SYNZIP5	SYNZIP6	SYNZIP15	ATF4	SYNZIP7
pair+line	A-B,C-D-E	SYNZIP7	ATF4	SYNZIP5	SYNZIP6	SYNZIP23
pair+line	A-B,C-D-E	SYNZIP3	SYNZIP4	SYNZIP19	SYNZIP22	ATF4
pair+line	A-B,C-D-E	SYNZIP2	SYNZIP1	SYNZIP21	SYNZIP4	SYNZIP3
pair+line	A-B,C-D-E	SYNZIP3	SYNZIP4	SYNZIP15	ATF4	SYNZIP7
pair+line	A-B,C-D-E	SYNZIP7	ATF4	SYNZIP9	FOS	SYNZIP17
pair+line	A-B,C-D-E	SYNZIP9	FOS	SYNZIP21	SYNZIP4	SYNZIP3
pair+line	A-B,C-D-E	SYNZIP7	ATF4	SYNZIP8	SYNZIP23	SYNZIP6
hub	A-B,A-C,A-D,A-E	SYNZIP23	SYNZIP12	SYNZIP18	SYNZIP16	SYNZIP6
hub	A-B,A-C,A-D,A-E	SYNZIP23	SYNZIP12	SYNZIP18	SYNZIP16	SYNZIP8
hub	A-B,A-C,A-D,A-E	SYNZIP23	SYNZIP12	SYNZIP18	SYNZIP16	BATF
hub	A-B,A-C,A-D,A-E	SYNZIP23	SYNZIP12	SYNZIP16	SYNZIP6	SYNZIP8
hub	A-B,A-C,A-D,A-E	SYNZIP23	SYNZIP12	SYNZIP16	SYNZIP6	BATF
hub	A-B,A-C,A-D,A-E	SYNZIP23	SYNZIP12	SYNZIP16	SYNZIP8	BATF
hub	A-B,A-C,A-D,A-E	SYNZIP23	SYNZIP18	SYNZIP16	SYNZIP6	SYNZIP8
hub	A-B,A-C,A-D,A-E	SYNZIP23	SYNZIP18	SYNZIP16	SYNZIP6	BATF
hub	A-B,A-C,A-D,A-E	SYNZIP23	SYNZIP18	SYNZIP16	SYNZIP8	BATF
hub	A-B,A-C,A-D,A-E	SYNZIP23	SYNZIP16	SYNZIP6	SYNZIP8	BATF
hub	A-B,A-C,A-D,A-E	SYNZIP23	SYNZIP18	SYNZIP12	SYNZIP6	SYNZIP8
hub	A-B,A-C,A-D,A-E	SYNZIP23	SYNZIP18	SYNZIP12	SYNZIP6	BATF
hub	A-B,A-C,A-D,A-E	SYNZIP23	SYNZIP18	SYNZIP12	SYNZIP8	BATF
hub	A-B,A-C,A-D,A-E	SYNZIP23	SYNZIP12	SYNZIP6	SYNZIP8	BATF
hub	A-B,A-C,A-D,A-E	SYNZIP23	SYNZIP18	SYNZIP21	SYNZIP6	SYNZIP8
hub	A-B,A-C,A-D,A-E	SYNZIP23	SYNZIP18	SYNZIP21	SYNZIP6	BATF
hub	A-B,A-C,A-D,A-E	SYNZIP23	SYNZIP18	SYNZIP21	SYNZIP8	BATF
hub	A-B,A-C,A-D,A-E	SYNZIP23	SYNZIP18	SYNZIP6	SYNZIP8	BATF
hub	A-B,A-C,A-D,A-E	SYNZIP23	SYNZIP21	SYNZIP6	SYNZIP8	BATF
6 nodes	**Motif**	**A**	**B**	**C**	**D**	**E**	**F**
line + pair	A-B-C-D, E-F	SYNZIP5	SYNZIP6	SYNZIP23	SYNZIP8	ATF4	SYNZIP7
line + pair	A-B-C-D, E-F	SYNZIP13	SYNZIP15	ATF4	SYNZIP7	SYNZIP5	SYNZIP6
3 pairs	A-B,C-D,E-F	SYNZIP9	FOS	ATF4	SYNZIP7	SYNZIP5	SYNZIP6
3 pairs	A-B,C-D,E-F	SYNZIP9	FOS	ATF4	SYNZIP7	SYNZIP4	SYNZIP3
hub	A-B,A-C,A-D,A-E,A-F	SYNZIP23	SYNZIP16	BATF	SYNZIP8	SYNZIP6	SYNZIP18
hub	A-B,A-C,A-D,A-E,A-F	SYNZIP23	SYNZIP16	BATF	SYNZIP8	SYNZIP6	SYNZIP12
hub	A-B,A-C,A-D,A-E,A-F	SYNZIP23	SYNZIP16	BATF	SYNZIP8	SYNZIP18	SYNZIP12
hub	A-B,A-C,A-D,A-E,A-F	SYNZIP23	SYNZIP16	BATF	SYNZIP6	SYNZIP18	SYNZIP12
hub	A-B,A-C,A-D,A-E,A-F	SYNZIP23	SYNZIP16	SYNZIP8	SYNZIP6	SYNZIP18	SYNZIP12
hub	A-B,A-C,A-D,A-E,A-F	SYNZIP23	SYNZIP12	BATF	SYNZIP8	SYNZIP6	SYNZIP18
hub	A-B,A-C,A-D,A-E,A-F	SYNZIP23	SYNZIP18	BATF	SYNZIP8	SYNZIP6	SYNZIP21

Table S4. Crystallographic data collection and refinement statistics.

Protein Data Set	SYNZIP6: SYNZIP5	SYNZIP1: SYNZIP2
Space Group	P 63	P 31
Cell dimensions *a*, *b*, *c*(Å) α, β, γ(°)	 82.7, 82.7, 150.6 90, 90, 120	 49.9, 49.9, 113.2 90, 90, 120
λ (Å)	0.97927	1.5418
Resolution (Å)	50 - 2.46	50 - 1.75
Rsym (%)[a,b]	10.9 (54.8)	3.8 (29.4)
# ref	21204	31354
Completeness (%)[a]	99.7 (99.3)	98.2 (90.7)
Redundancy[a]	5.8 (5.4)	4.6 (2.8)
# dimers/ASU	4	3
Twin law	h,-h-k,-l	-k,-h,-l
Twin fraction	0.324	0.392
R_{work}/R_{free}(%)[c]	21.2/25.8	19.0/22.8

[a]Values in parentheses refers to data in the highest resolution shell

[b]$R_{sym} = \Sigma_h\Sigma_j |I_j(h) - \langle I(h)\rangle| / \Sigma_h\Sigma_j \langle I(h)\rangle$, where $I_j(h)$ is the j^{th} reflection of index h and $\langle I(h)\rangle$ is the average intensity of all observations of I(h)

[c]$R_{work} = \Sigma_h |F_{obs}(h) - F_{calc}(h)| | / \Sigma_h |F_{obs}(h)|$, calculated over the 95% of the data in the working set. R_{free} equivalent to R_{work} except calculated over the 5% of the data assigned to the test set